

Applied and Environmental Microbiology

CosR is a repressor of compatible solute biosynthesis and transporter systems

Gwendolyn J. Gregory, Daniel P. Morreale, and E. Fidelma Boyd*

Department of Biological Sciences, University of Delaware, Newark, DE, 19716

Corresponding author*

E. Fidelma Boyd

Department of Biological Sciences

341 Wolf Hall, University of Delaware

Newark, DE 19716

Phone: (302) 831-1088. Fax: (302) 831-2281 Email: fboyd@udel.edu

Abstract

Bacteria accumulate small, organic compounds, called compatible solutes, via uptake from the environment or biosynthesis from available precursors to maintain the turgor pressure of the cell in response to osmotic stress. *Vibrio parahaemolyticus* has biosynthesis pathways for the compatible solutes ectoine (*ectABCasp_ect*) and glycine betaine (*betIBAprWXV*), four betaine-carnitine-choline transporters (*bcct1-bcct4*) and a second ProU transporter (*proVWX*). Most of these systems are induced in high salt. CosR, a MarR-type regulator, which is divergently transcribed from *bcct3*, was previously shown to be a direct repressor of *ectABCasp_ect* in *Vibrio* species. In this study, we investigated the role of CosR in glycine betaine biosynthesis and compatible solute transporter gene regulation. Expression analyses demonstrated that *betIBAprWXV*, *bcct1*, *bcct3*, and *proVWX* are repressed in low salinity. Examination of an in-frame *cosR* deletion mutant shows induced expression of these systems in the mutant at low salinity compared to wild-type. DNA binding assays demonstrate that purified CosR binds directly to the regulatory region of each system. In *Escherichia coli* GFP reporter assays, we demonstrate that CosR directly represses transcription of *betIBAprWXV*, *bcct3*, and *proVWX*. Similar to *V. harveyi*, we show *betIBAprWXV* is positively regulated by the LuxR homolog OpaR. Bioinformatics analysis demonstrates that CosR is widespread within the genus, present in over 50 species. In several species, the *cosR* homolog was clustered with the *betIBAprWXV* operon, which again suggests the importance of this regulator in glycine betaine biosynthesis. Incidentally, in four *Aliivibrio* species that contain ectoine biosynthesis genes, we identified another MarR-type regulator, *ectR*, clustered with these genes, which suggests the presence of a novel ectoine regulator. Homologs of EctR in this genomic context were present in *A. fischeri*, *A. finisterrensis*, *A. sifiae* and *A. wodanis*.

40 **Importance**

41 *Vibrio parahaemolyticus* can accumulate compatible solutes via biosynthesis and transport,
 42 which allow the cell to survive in high salinity conditions. There is little need for compatible
 43 solutes under low salinity conditions, and biosynthesis and transporter systems are repressed.
 44 However, the mechanism of this repression is not fully elucidated. CosR plays a major role in the
 45 repression of multiple compatible solute systems in *V. parahaemolyticus* as a direct negative
 46 regulator of ectoine and glycine betaine biosynthesis systems and four transporters. Homology
 47 analysis suggests that CosR functions in this manner in many other *Vibrio* species. In *Aliivibrio*
 48 species, we identified a new MarR family regulator EctR that clusters with the ectoine
 49 biosynthesis genes.

Introduction

Halophilic bacteria such as *Vibrio parahaemolyticus* encounter a range of osmolarities in the environment. To combat the loss of turgor pressure due to efflux of water in high osmolarity conditions, bacteria have developed a strategy that involves the accumulation of compatible solutes in the cell (1-3). Compatible solutes, as the name suggests, are organic compounds that are compatible with the molecular machinery and processes of the cell, and include compounds such as ectoine, glycine betaine, trehalose, glycerol, proline, glutamate, and carnitine, among others (1, 4-9). Compatible solutes are taken up from the environment or synthesized from various precursors in response to osmotic stress, which allows cells to continue to grow and divide even in unfavorable environments (2, 4, 10, 11).

Vibrio parahaemolyticus possesses compatible solute biosynthesis pathways for ectoine and glycine betaine (12). Ectoine biosynthesis is *de novo* in *V. parahaemolyticus*, requiring aspartic acid as the precursor, which can be supplied by the cell (13). Aspartic acid is converted to ectoine by four enzymes, EctA, EctB, EctC and Asp_Ect, encoded by the operon *ectABCasp_ect* (14). Ectoine biosynthesis begins with L-aspartate- β -semialdehyde, which is also pivotal to bacterial amino acid and cell wall synthesis (14). Asp_Ect is a specialized aspartokinase dedicated to the ectoine pathway that, among Proteobacteria, is present only in alpha, gamma and delta species (15). Searches of the genome database demonstrated that ectoine biosynthesis genes are present in nearly 500 species. Of these, nearly a third also produce 5-hydroxyectoine by the action of an additional gene product, ectoine hydroxylase, encoded by *ectD* (16). A recent study has shown that in *V. parahaemolyticus* the quorum sensing response regulator OpaR is a negative regulator of *ect* gene expression (17). It was also shown that in this

species, similar to *V. cholerae*, a multiple antibiotic resistance (MarR)-type regulator named CosR is a repressor of *ectABCasp_ect* (17, 18).

Production of glycine betaine takes place in a two-step oxidation from the precursor choline, which is acquired exogenously. *De novo* biosynthesis of glycine betaine has been identified in only a few species of halophilic bacteria (19-24). The two-step oxidation proceeds with choline conversion to glycine betaine by the products of two genes *betB* and *betA*, which encode betaine-aldehyde dehydrogenase and choline dehydrogenase, respectively (25, 26). In *E. coli*, these genes are encoded by the operon *betIBA*, with the regulator BetI shown to repress its own operon (27, 28). In all *Vibrio* species that biosynthesize glycine betaine, the *betIBA* genes are in an operon with the *proXWV* genes, which encode a ProU transporter (12, 13, 29). Regulation of glycine betaine biosynthesis has been studied in several species, but few direct mechanisms of regulation have been shown beyond BetI (27, 28, 30-33). In *V. harveyi*, a close relative of *V. parahaemolyticus*, *betIBaproXWV* was shown to be positively regulated by the quorum sensing master regulator LuxR (32-33).

It is energetically favorable to the cell to uptake compatible solutes from the environment rather than to biosynthesize them, and Bacteria and Archaea encode multiple osmoregulated transporters (9, 34-39). ATP-binding cassette (ABC) transporters are utilized to import exogenous compatible solutes into the cell and include ProU (encoded by *proVWX*) in *E. coli* and *Pseudomonas syringae*, OpuA in *Lactococcus lactis* and *B. subtilis*, and OpuC in *P. syringae* (39-44). *V. parahaemolyticus* encodes two putative ProU transporters of the ABC transporter family, one on each chromosome. ProU1 is encoded on chromosome 1 by *proVWX* (VP1726-VP1728) and ProU2 is encoded on chromosome 2 by the *betIBaproXWV* operon (VPA1109-VPA1114) (12). ProU1 is a homolog of the *E. coli* K-12 ProU, which in this species was shown

to bind glycine betaine with high affinity (41, 45, 46). ProU2 is a homolog of the *P. syringae* *proVXW* (12).

The betaine-carnitine-choline transporters (BCCTs) are single component transporters, the first of which, BetT, discovered in *E. coli*, was shown to transport choline with high-affinity and is divergently transcribed from *betIBA* (47, 48). *Vibrio parahaemolyticus* encodes four BCCTs, three, BCCT1-BCCT3 (VP1456, VP1723, VP1905), on chromosome 1 and one, BCCT4 (VPA0356), on chromosome 2 (12). This is a typical complement of *bcct* genes present among members of the Campbellii clade, which includes *V. alginolyticus*, *V. campbellii*, *V. harveyi* and *V. parahaemolyticus*, amongst others (Naughton et al., 2009). The *bcct2* (VP1723) gene is the only *bcct* gene that is not induced by high salinity in *V. parahaemolyticus* (13). All four BCCT transporter were shown to transport glycine betaine amongst others (29). A study in *V. cholerae* demonstrated that a *bcct3* homolog is repressed by the regulator CosR and deletion of the *cosR* gene also affected biofilm formation and motility in this species (18).

In this study, we examined the broader role of CosR in the regulation of glycine betaine biosynthesis and compatible solute transport gene expression in *V. parahaemolyticus*. First, we examined expression of genes encoding osmotic stress response systems in low salinity and used quantitative real-time PCR to determine expression of these genes in a $\Delta cosR$ deletion mutant. We then determined whether CosR was a direct regulator using DNA binding assays and an *E. coli* plasmid-based reporter assay. We also examined whether *betIBA_{proXWV}* was under the control of the LuxR homolog OpaR in *V. parahaemolyticus*, similar to what was shown in *V. harveyi*. We investigated the distribution of CosR and its genome context among *Vibrionaceae*. Our data indicate that CosR is a key regulator of the osmotic stress response in *V.*

parahaemolyticus under low salinity conditions. Distribution of CosR is widespread, and similar genomic context suggests CosR repression of compatible solutes is common among *Vibrio*.

Results

Compatible solute biosynthesis and transport genes are downregulated in low salinity. We have previously shown that *V. parahaemolyticus* does not produce compatible solutes ectoine and glycine betaine during growth in minimal media (M9G) supplemented with 1% NaCl (M9G1%) (12, 13). Here we quantified expression levels of both biosynthesis operons in M9G1% or M9G3%. RNA was isolated from exponentially growing wild-type *V. parahaemolyticus* RIMD2210633 cells, at optical density 595 nm (OD₅₉₅) 0.45, after growth in M9G1% or M9G3%. Real time quantitative PCR (qPCR) was performed to determine relative expression levels. Expression analysis shows that ectoine biosynthesis genes *ectA* and *asp_ect* are differentially expressed in M9G1% as compared to expression in M9G3%. *ectA* is significantly downregulated 794.6-fold and *asp_ect* is significantly downregulated 204.9-fold in M9G1% (Fig. 1A). The *betIABproXWV* operon is also significantly repressed in M9G1%, with fold changes of 25.8-fold, 22-fold, 33.7-fold, and 52.8-fold for *betI*, *betB*, *proX*, and *proW*, respectively (Fig. 1B).

We determined the expression levels of *bcct* genes in *V. parahaemolyticus* in both M9G1% and M9G3%. Expression of *bcct1*, *bcct3*, and *bcct4* are significantly repressed in M9G1%, 500-fold, 71.4-fold, and 11.6-fold, respectively, when compared with expression in M9G3% (Fig. 1C). The *bcct2* gene remained unchanged. We previously reported that *bcct2* is not induced by salinity (29), and our data indicates that it has a basal level of transcription in the cell based on similar Ct values in both salinities tested (data not shown). We then examined the

expression pattern of the ProU1 transporter genes in *V. parahaemolyticus*. The *proV1* gene is significantly repressed in M9G1%, with a 2,786-fold change as compared to M9G3% (Fig. 1C). Overall, the data demonstrates osmoregulation of ectoine and glycine betaine biosynthesis genes and transporter genes *bcct1*, *bcct3*, *bcct4* and *proVWX*.

CosR represses compatible solute biosynthesis and transport genes in low salinity. Next, we wanted to determine how these compatible solute systems are repressed in *V. parahaemolyticus*. Since we know CosR is a repressor of ectoine biosynthesis genes, we wondered whether it played a broader role in repression of the osmotic stress response genes, *betIBAproXWV* operon, *proVWX*, and *bcct* transporters, in low salt conditions. We examined expression of these genes in wild-type and an in-frame deletion mutant of *cosR*. RNA was isolated from the $\Delta cosR$ mutant strain at mid-exponential phase (OD₅₉₅ 0.45) after growth in M9G1% and compared to wild-type RIMD2210633 grown under identical conditions. Using qPCR analysis, we determined the expression levels of *ectA* and *asp_ect* and show they are significantly induced, 818.5-fold and 308.2-fold, respectively, in a $\Delta cosR$ mutant compared to wild-type in M9G1% (Fig. 2A). Next, we examined expression levels of *betIBAproXWV* after growth in M9G1% in the $\Delta cosR$ and wild-type strains using qPCR. The *betI*, *betB*, *proX2* and *proW2* genes are significantly induced in the $\Delta cosR$ mutant with *betI* expressed 13.75-fold, *betB* 10.18-fold, *proX2* 8.23-fold, and *proW2* 16.38-fold more than in the wild-type strain (Fig. 2B). Similarly, we examined levels of the *bcct* genes and *proV1* in a $\Delta cosR$ mutant versus the wild-type in M9G1%. Relative expression levels of *bcct1* are 155.66-fold higher and levels of *bcct3* are 34.97-fold higher than wild-type levels, while levels of *bcct2* and *bcct4* are unchanged (Fig. 2C). The *proV1* gene is induced 379.5-fold in the $\Delta cosR$ mutant over the wild-type strain (Fig. 2C). In sum, these data

demonstrate that CosR is a repressor of *ectABCasp_ect*, *betIBAprOXWV*, *bcct1*, *bcct3* and *proVWX* under low salinity conditions.

CosR binds directly to the promoter of the *betIBAprOXWV* operon and represses transcription. Previously, we found that CosR binds to the regulatory region of the ectoine biosynthesis operon and represses transcription (17). To determine whether CosR regulation of the glycine betaine biosynthesis operon is also direct, we performed DNA binding assays with purified CosR protein and DNA probes of the regulatory region of this operon. The regulatory region was split into five overlapping probes, *PbetI* probes A-E, of sizes 125-bp, 112-bp, 142-bp, 202-bp, and 158-bp (Fig. 3A). CosR bound to probe A, which is directly upstream of the start codon for *betI*, and it also bound to probes B and D (Fig. 3B). CosR did not bind to probes C and E, demonstrating specificity of CosR binding (Fig. 3B).

To demonstrate that direct binding by CosR results in transcriptional repression of the *betIBAprOXWV* operon, we performed a GFP-reporter assay in *E. coli* strain MKH13. Full-length *cosR* was expressed from a plasmid (pBBR*cosR*) in the presence of a *gfp*-expressing reporter plasmid under the control of the glycine betaine biosynthesis system regulatory region (*P_{betI}-gfp*). Relative fluorescence and OD₅₉₅ were measured after overnight growth in M9G1%. Specific fluorescence was calculated by normalizing to OD and compared to specific fluorescence in a strain with an empty expression vector (pBBR1MCS) that also contained the *P_{betI}-gfp* reporter plasmid. The activity of the *P_{betI}-gfp* reporter was significantly repressed 4.84-fold as compared to the empty vector strain (Fig. 3C). This indicates that CosR directly represses transcription of the *betIBAprOXWV* genes.

CosR binds directly to the promoter of *bcct1* and *bcct3*. Next, we wanted to investigate whether CosR repression of *bcct1* and *bcct3* was direct. We designed probes upstream of the translational start for *bcct1* and *bcct3*. The 291-bp regulatory region of *Pbcct1*, which includes 15-bp of *bcct1* and 276-bp of the intergenic region, was split into three overlapping probes, *Pbcct1* probes A, B, and C, 120-bp, 110-bp, and 101-bp, respectively (Fig. 4A). DNA binding assays were performed with increasing concentrations of CosR. CosR bound directly to the *Pbcct1* probe B (Fig. 4B) but did not bind to the other probes tested, indicating that regulation by CosR is direct and binding is specific. We then performed GFP reporter assays in *E. coli* using a GFP expression plasmid under the control of the regulatory region of *bcct1*. and a CosR expression plasmid (pBBR*cosR*). Specific fluorescence in the presence of CosR was compared to a strain with empty expression vector (pBBR1MCS). The activity of the *P_{bcct1}-gfp* reporter was not significantly different than the strain harboring empty expression vector (Fig. 4C), indicating that CosR does not directly repress *bcct1*.

Two overlapping probes designated *Pbcct3* probe A and B, 108-bp and 107-bp, respectively, were designed encompassing 196-bp of the regulatory region of *bcct3* (Fig. 5A). Because *bcct3* is divergently transcribed from *cosR*, we used approximately half of the regulatory region for the *Pbcct3* EMSA. An EMSA showed that CosR bound directly to the *Pbcct3* probe A, which is proximal to the start of the gene, but not probe B (Fig. 5B). We then performed GFP reporter assays in *E. coli* using a GFP expression plasmid under the control of the regulatory region of *bcct3*, utilizing the entire 397-bp intergenic region between *bcct3* and *cosR*. Transcriptional activity of the *P_{bcct3}-gfp* reporter is significantly repressed in a CosR-expressing strain, indicating that CosR directly represses transcription of *bcct3* (Fig. 5C). In addition, we showed that CosR does not bind to the regulatory region of *bcct2* and *bcct4* (Fig.

5D), which is in agreement with the *cosR* mutant expression data (Fig. 2C). These data suggest that *bcct2* and *bcct4* are under the control of a yet to be described regulator.

CosR binds directly to the *proVWX* regulatory region. We also examined direct regulation of the *proVWX* operon on chromosome 1 by CosR. The regulatory region upstream of the *proVI* gene was divided into four probes, 160-bp, 134-bp, 108-bp and 109-bp (Fig. 6A). A DNA binding assay was performed with increasing concentrations of CosR and 30 ng of each probe. A shift in the DNA bands of probe D, which is proximal to the start codon of *proVI*, indicates that CosR binds directly to this region (Fig. 6B). CosR did not bind to the other probes tested, indicating that CosR binding is specific.

We also performed a GFP-reporter assay in *E. coli* utilizing the *cosR* expression plasmid (pBBRCosR) and a GFP reporter plasmid under the control of the *proVWX* regulatory region (P_{proVI} -*gfp*). We found that in a CosR-expressing strain, expression of the P_{proVI} -*gfp* reporter was significantly repressed when compared to an empty expression vector strain (Fig. 6C). This indicates that CosR is a direct repressor of the *proVWX* operon.

CosR is a MarR-type regulator that does not participate in an autoregulatory feedback loop. In *V. cholerae*, expression levels of *cosR* are upregulated in 0.5 M NaCl as compared to levels in 0.2 M NaCl (18). It was suggested that one reason for the upregulation of *cosR* in higher salinity could be that it is involved in an autoregulatory feedback loop (18). In *V. parahaemolyticus*, we found that levels of *cosR* are not significantly upregulated in moderate salinity (3% NaCl) as compared to low salinity (1% NaCl) (data not shown). We have already shown that CosR binds to the intergenic region between *bcct3* and *cosR*, but the binding site location is proximal to the start codon of *bcct3*, more than 300 bp upstream of the *cosR* gene (Fig. 5A & B). Therefore, to investigate CosR autoregulation, we designed two probes, 105-bp

and 142-bp, which comprise a 220-bp portion of the regulatory region upstream of *cosR* (VP1906) (Fig. 7A) and used this in a DNA binding assay with various concentrations of purified CosR (Fig. 7B). There are no shifts observed in the binding assay, indicating that CosR does not bind (Fig. 7B). We then performed a GFP reporter assay in *E. coli*, utilizing the entire 397-bp intergenic region between *bcct3* and *cosR*, to determine if CosR directly represses transcription of its own gene. The transcriptional activity of P_{cosR} -*gfp* in the presence of CosR was not significantly different from the empty-vector strain (Fig. 7C). We therefore conclude that under these conditions, in *V. parahaemolyticus* CosR does not autoregulate, and that the CosR binding site proximal to the *bcct3* gene does not affect transcription of the *cosR* gene.

BetI represses its own operon in the absence of choline. Previously, it was shown that BetI represses its own operon in several bacterial species and this repression is relieved in the presence of choline (27, 31, 32). To demonstrate BetI regulates its own operon in *V. parahaemolyticus*, we performed a plasmid-based GFP reporter assay utilizing the P_{betI} -*gfp* reporter in RIMD2210633 strain and a $\Delta betI$ mutant strain. Strains were grown overnight in M9G3%, with and without choline, and specific fluorescence was calculated. Expression of the reporter is significantly induced in the $\Delta betI$ mutant when no choline is present, indicating that BetI is a negative regulator of its own operon (Fig. 8A). In the presence of choline, there is no longer a significant difference in reporter activity between the wild-type strain and the $\Delta betI$ mutant strain, indicating that repression by BetI is relieved (Fig. 8B).

To determine whether regulation of *betIBA*_{proXWV} by BetI is direct, we performed a GFP reporter assay in *E. coli* MKH13 strain. The P_{betI} -*gfp* reporter utilized in our *in vivo* reporter assay was introduced into the *E. coli* MKH13 strain (which lacks its own *betIBA* operon) along

with an expression vector harboring full-length *betI* under the control of an IPTG-inducible promoter. In the BetI-expressing strain, P_{betI} -*gfp* expression was significantly repressed, indicating that BetI is a direct repressor of its own operon in *V. parahaemolyticus* (Fig. 8C).

The LuxR homolog OpaR is a positive regulator of *betIBAproXWV* in *V. parahaemolyticus*.**

It was demonstrated in *V. harveyi* that LuxR, the quorum sensing master regulator, induces *betI**BAproXWV* expression and that this regulation is direct (32). We examined expression of the P_{betI} -*gfp* reporter in wild-type and the $\Delta opaR$ mutant in *V. parahaemolyticus*. Expression of the reporter is significantly repressed in $\Delta opaR$, indicating that OpaR is a positive regulator of the glycine betaine biosynthesis operon in *V. parahaemolyticus* (Fig. 9A). We also examined whether regulation of P_{betI} by OpaR was direct utilizing an EMSA with purified OpaR protein. The P_{betI} probes A-E used previously in the CosR EMSA (Fig. 3A) were incubated with purified OpaR. OpaR bound to all P_{betI} probes, indicating that regulation of *betI**BAproXWV* by OpaR is direct (Fig. 9B).

Distribution of compatible solute biosynthesis and transport systems in *Vibrionaceae*.

CosR, a MarR family regulator, in *V. parahaemolyticus* is a 158 amino acid protein that is divergently transcribed from *bcct3* on chromosome 1. Our BLAST analysis showed that a CosR homolog is present in over 50 *Vibrio* species and in all cases the *cosR* homolog was divergently transcribed from a *bcct* transporter. Within these *Vibrio* species, homology ranged from 98% to 73% amino acid identity. We found that in *V. splendidus*, *V. crassostreae*, *V. cyclitrophicus*, *V. celticus*, *V. lentus* and *Aliivibrio wodanis*, the CosR homolog is present directly downstream of the *betI**BAproXWV* operon on chromosome 2 (**Fig. 10**). CosR in these species share ~73-75% amino acid identity with CosR in *V. parahaemolyticus*. In *V. tasmaniensis* strains and *Vibrio* sp.

MED222, the CosR homolog is also downstream of the betaine biosynthesis operon and the operon for ectoine biosynthesis clusters in the same genome location (**Fig. 10**). In two *Aliivibrio wodanis* strains, AWOD1 and 06/90/160, *cosR* homologs were clustered with putative transporters and the glycine betaine biosynthesis operon. In all strains of *Aliivibrio fischeri*, the *cosR* homolog (which shares 73% amino acid identity with CosR from *V. parahaemolyticus*) clusters with two uncharacterized transporters. However, a second MarR family regulator, a 141 amino acid protein, which we name *ectR*, clusters with the ectoine biosynthesis genes in this species. EctR shares only 31% identity with less than 60% query coverage to CosR from *V. parahaemolyticus* and a similar level of low amino acid identity to EctR1 from *Methylmicrobium alcaliphilum*. EctR was also clustered with the *ectABCasp_ect* genes in all strains of *Aliivibrio finisterrensis*, *Aliivibrio sifiae*, and most *A. wodanis* strains. Thus, in *Aliivibrio* species, it appears that the ectoine gene cluster has a new uncharacterized regulator of the MarR family, which was confined to this group.

Discussion

Here we have shown that the compatible solute biosynthesis and transport genes are downregulated in *V. parahaemolyticus* in low salinity. Our genetic analysis, binding analysis, and reporter assays demonstrate that the transcriptional regulator CosR is a direct repressor of *betIBAproXWV*, *bcct3*, and *proVWX* in low salinity. Additionally, we show that under the conditions tested, CosR is not autoregulated in *V. parahaemolyticus*. Our bioinformatics analysis indicates that CosR repression of compatible solute systems is likely widespread within the *Vibrio* genus.

Although CosR binds directly to the regulatory region of *bcct1*, transcription was not directly repressed in our reporter assay. Based on our expression data combined with our DNA-

binding assays, we speculate it is probable that CosR also directly represses *bcct1* expression, but we could not detect significant differences between the CosR- and empty vector-expressing strains due to the low level of activation of the *bcct1* regulatory region in *E. coli*.

CosR characterized from *Vibrio* species show ~50% amino acid identity to EctR1, a MarR-type regulator in the halotolerant methanotroph *Methylmicrobium alcaliphilum* (49). In this species, *ectR1* is divergently transcribed from the same promoter as *ectABC-asp_ect*. Mustakhimov and colleagues showed that EctR1 repressed expression of the *ectABC-ask* operon in response to low salinity (49). Purified EctR1 bound specifically to the promoter of *ectABC-ask*, indicating direct regulation by EctR1 (49). EctR repression of the ectoine biosynthesis genes was also shown in both *Methylophaga alcalica* and *Methylophaga thalassica*, two moderately halophilic methylotrophs (50, 51). In *V. cholerae*, CosR was also identified as a repressor of ectoine biosynthesis genes though it does not cluster with *ectABC-asp_ect* (18). The *cosR* gene in *V. cholerae* is divergently transcribed from the *opuD* gene (a *bcct3* homolog), which is also repressed by CosR (18). Similarly, in *V. parahaemolyticus*, the *cosR* (VP1906) homolog is divergently transcribed from *bcct3* (VP1905). In this species, we demonstrated previously that CosR is a direct negative regulator of *ectABCasp_ect* and show here that it directly represses *bcct3* (17). Our bioinformatics analysis found that the CosR homolog is divergently transcribed from *bcct3* in over 50 *Vibrio* species demonstrating conservation of genomic context suggesting functional conservation. In several *Vibrio* species the CosR homolog was clustered with the *betIBAproXWV* operon, which is further suggestive of its role in regulation of compatible solute biosynthesis among *Vibrio* species. Incidentally, in *V. tasmaniensis* LGP32 (formerly *V. splendidus* LGP32) and *Vibrio* MED222, the ectoine gene cluster was present in the same genome region as the *betIBAproXWV-cosR* cluster.

CosR and EctR1 are members of the MarR family of transcriptional regulators, first characterized in *E. coli*, which are important regulators of a number of cellular responses, typically responding to a change in the external environment (52-54). The literature suggests that MarR-type regulators form dimers and bind to a 20-45 bp pseudo-palindromic site in the intergenic region of genes it controls (52, 55-57). The activity of MarR-type regulators can be modulated by the presence of a chemical signal, either a ligand, metal ion, or reactive oxygen species. Binding of these signals causes the protein to undergo a conformational change, thereby affecting DNA binding capability (52, 58, 59). We modeled a CosR homodimer using SWISS-MODEL and did not identify a ligand binding pocket. In *V. cholerae*, CosR activity is not affected by the presence of exogenous compatible solutes including ectoine, glycine betaine and proline, and *opuD* (*bcct* homolog) transcripts were unchanged in a *cosR* mutant. Hence, the environmental or cellular signals that modulate the activity of CosR remain unknown, as was noted by Czech and colleagues (60). Interestingly, our modelling of the EctR regulator identified in *Aliivibrio* species indicated it also does not have a ligand-binding pocket.

Autoregulation was shown for several MarR family regulators, including *ectR1* in *M. alcaliphilum* (49, 52). It was suggested previously that CosR maybe involved in an autoregulatory feedback loop in *V. cholerae* (18). In *V. parahaemolyticus* we show CosR does not bind to its own regulatory region, and our reporter assay suggests that CosR does not autoregulate. It is interesting to note that EctR1 participates in an autoregulatory feedback loop in *M. alcaliphilum* but not in *M. thalassica* (51, 61).

Ectoine biosynthesis is present in all halophilic *Vibrio* species and is essential for growth in high salt in the absence of compatible solute uptake (13). However, compatible solutes are not required under low salinity conditions. The physiological role of CosR repression of compatible

solute biosynthesis in low salinity is likely to protect levels of key intracellular metabolites such as glutamate, acetyl-CoA, and oxaloacetate, all of which are affected by ectoine biosynthesis (62, 63).

Similar to ectoine biosynthesis gene expression, few direct regulators of glycine betaine biosynthesis genes have been identified. In *E. coli*, expression of *betIBA* was repressed by BetI and repression was relieved in the presence of choline (27). BetI was shown to directly regulate transcription at this locus via DNA binding assays (28). ArcA was shown to repress the *bet* operon under anaerobic conditions in *E. coli*, although direct binding was not shown (27). In *Vibrio harveyi*, it was shown that *betIBAprWXV* were repressed 2- to 3-fold when *betI* was overexpressed from a plasmid. Purified BetI bound directly to the regulatory region of the *betIBAprWXV* operon in DNA binding assays (32, 33). In these studies, it was also shown that the quorum sensing response regulator LuxR, along with the global regulator IHF, activated expression of *betIBAprWXV* (32, 33). Here we have shown that BetI represses its own operon in *V. parahaemolyticus*, as expected, and we identified a novel regulator of glycine betaine biosynthesis genes, CosR, which directly represses under low salinity conditions. We also confirm that, similar to *V. harveyi*, the quorum sensing master regulator OpaR induced *betIBAprWXV* expression in *V. parahaemolyticus* and this regulation is direct.

Biosynthesis of compatible solutes is an energetically costly process for bacteria (35). *V. parahaemolyticus* does not accumulate compatible solutes in low salinity (12, 13, 29), and therefore the transcription of biosynthesis and transport genes is unnecessary. CosR represses the genes involved in the osmotic stress response in *V. parahaemolyticus* in low salinity conditions. The high conservation of the CosR protein across *Vibrio* species and its genomic context indicates that regulation by CosR of compatible solute systems is widespread in bacteria.

Materials and Methods:

Bacterial strains, media and culture conditions. Listed in Table 1 are all strains and plasmids used in this study. A previously described streptomycin-resistant clinical isolate of *V. parahaemolyticus*, RIMD2210633, was used as the wild-type strain (64)Makino et al., 2003). *V. parahaemolyticus* strains were grown in either lysogeny broth (LB) (Fisher Scientific, Fair Lawn, NJ) supplemented with 3% NaCl (wt/vol) (LBS) or in M9 minimal medium (47.8 mM Na₂HPO₄, 22 mM KH₂PO₄, 18.7 mM NH₄Cl, 8.6 mM NaCl) (Sigma-Aldrich, USA) supplemented with 2 mM MgSO₄, 0.1 mM CaCl₂, 20 mM glucose as the sole carbon source (M9G) and 1% or 3% NaCl (wt/vol) (M9G1%, M9G3%). *E. coli* strains were grown in LB supplemented with 1% NaCl (wt/vol) or M9G1% where indicated. *E. coli* β2155, a diaminopimelic acid (DAP) auxotroph, was supplemented with 0.3 mM DAP and grown in LB 1% NaCl. All strains were grown at 37°C with aeration. Antibiotics were used at the following concentrations (wt/vol) as necessary: ampicillin (Amp), 50 µg/ml; chloramphenicol (Cm), 12.5 µg/ml; tetracycline (Tet), 1 µg/mL; and streptomycin (Str), 200 µg/ml. Choline was added to media at a final concentration of 1 mM, when indicated.

Construction of the *betI* deletion mutant. An in-frame *betI* (VPA1114) deletion mutant was constructed as described previously (17). Briefly, the Gibson assembly protocol, using NEBuilder HiFi DNA Assembly Master Mix (New England Biolabs, Ipswich, MA), followed by allelic exchange, was used to generate an in-frame 63-bp truncated, non-functional *betI* gene (65, 66). Two fragments, AB and CD, were amplified from the RIMD2210633 genome using primers listed in Table 2. These were ligated with pDS132, which had been digested with SphI, via Gibson assembly to produce suicide vector pDS132 with a truncated *betI* allele (pDSΔ*betI*). pDSΔ*betI* was transformed into *E. coli* strain β2155 λ*pir*, followed by conjugation with *V.*

parahaemolyticus. The suicide vector pDS132 must be incorporated into the *V. parahaemolyticus* genome via homologous recombination, as *V. parahaemolyticus* lacks the *pir* gene required for replication of the vector. Growth without chloramphenicol induces a second recombination event which leaves behind either the truncated mutant allele or the wild-type allele. Colonies were plated on sucrose for selection, as pDS132 harbors a *sacB* gene, which makes sucrose toxic to cells still carrying the plasmid. Healthy colonies were screened via PCR and sequenced to confirm an in-frame deletion of the *betI* gene.

RNA isolation and qPCR. *Vibrio parahaemolyticus* RIMD2210633 and $\Delta cosR$ were grown with aeration at 37 °C overnight in LBS. Cells were pelleted, washed twice with 1X PBS, diluted 1:50 into M9G3% or M9G1% and grown with aeration to mid-exponential phase (OD₅₉₅ 0.45). RNA was extracted from 1 mL of culture using Trizol, following the manufacturer's protocol (Invitrogen, Carlsbad, CA). The samples were treated with Turbo DNase (Invitrogen), followed by heat inactivation of the enzyme as per manufacturer's protocol. Final RNA concentration was quantified using a Nanodrop spectrophotometer (Thermo Scientific, Waltham, MA). 500 ng of RNA were used for cDNA synthesis by priming with random hexamers using SSIV reverse transcriptase (Invitrogen). Synthesized cDNA was diluted 1:25 and used for quantitative real-time PCR (qPCR). qPCR experiments were performed using PowerUp SYBR master mix (Life Technologies, Carlsbad, CA) on an Applied Biosystems QuantStudio6 fast real-time PCR system (Applied Biosystems, Foster City, CA). Reactions were set up with the following primer pairs listed in Table 2: VPbcct1Fwd/Rev, VPbcct2Fwd/Rev, VPbcct3Fwd/Rev, VPbcct4Fwd/Rev, VPectAFwd/Rev, VPasp_ectFwd/Rev, VPproV1Fwd/Rev, VPAbetIFwd/Rev, VPAbetBFwd/Rev, VPaproXFwd/Rev, VPaproWFwd/Rev, and 16SFwd/Rev for normalization. Expression levels were quantified using cycle threshold (CT) and were

normalized to 16S rRNA. Differences in gene expression were determined using the $\Delta\Delta CT$ method (67).

Protein purification of CosR. CosR was purified as described previously (17). Briefly, full-length *cosR* (VP1906) was cloned into the protein expression vector pET28a (+) containing an IPTG-inducible promoter and a C-terminal 6x-His tag (Novagen). Expression of CosR-His was then induced in *E. coli* BL21 (DE3) with 0.5 mM IPTG at OD₅₉₅ of 0.4 and grown overnight at room temperature. Cells were harvested, resuspended in lysis buffer (50 mM NaPO₄, 200 mM NaCl, 20 mM imidazole buffer [pH 7.4]) and lysed using a microfluidizer. CosR-His was bound to a Ni-NTA column and eluted with 50 mM NaPO₄, 200 mM NaCl, 500 mM imidazole buffer [pH 7.4] after a series of washes to remove loosely bound protein. Protein purity was determined via SDS-PAGE. OpaR was purified as described previously (68).

Electrophoretic Mobility Shift Assay. Five overlapping DNA fragments, designated *PbetI* probe A (125-bp), probe B (112-bp), probe C (142-bp), probe D (202-bp) and probe E (158-bp), were generated from the *betIBAproXWV* regulatory region (includes 36-bp of the coding region and the 594-bp upstream intergenic region) using primer sets listed in Table 2. Three overlapping DNA fragments, designated *PbcctI* probe A (120-bp), probe B (110-bp), and probe C (101-bp), were generated from the *bcctI* regulatory region (includes 15-bp of the coding region and the 276-bp upstream intergenic region) using primer sets listed in Table 2. Two overlapping DNA fragments, designated *Pbcct3* probe A (108-bp) and probe B (107-bp), were generated from the *bcct3* regulatory region (includes 17 bp of the coding region and 179-bp of the upstream intergenic region) using primer sets listed in Table 2. Four overlapping DNA fragments, designated *PproVI* probe A (160-bp), probe B (134-bp), probe C (108-bp), and probe D (109-

bp), were generated from the *proVI* regulatory region (includes 9 bp of the coding region and the 438-bp upstream intergenic region) using primer sets listed in Table 2. Fragments designated *Pbcct2* (233-bp) and *Pbcct4* (244-bp) were generated from the *bcct2* and *bcct4* regulatory regions, respectively, using primers listed in Table 2. Two overlapping DNA fragments, designated *PcosR* probe A (105-bp) and probe B (142-bp), were generated from the *cosR* regulatory region (includes 4-bp of the coding region and 216 bp of the upstream intergenic region) using primer sets listed in Table 2. The concentration of purified CosR-His and OpaR was determined using a Bradford assay. CosR or OpaR was incubated for 20 minutes with 30 ng of each DNA fragment in a defined binding buffer (10 mM Tris, 150 mM KCl, 0.5 mM dithiothreitol, 0.1 mM EDTA, 5% polyethylene glycol [PEG] [pH 7.9 at 4°C]). A 6% native acrylamide gel was pre-run for 2 hours at 4°C (200 V) in 1 X TAE buffer. Gels were loaded with the DNA:protein mixtures (10 µL), and run for 2 hours at 4°C (200 V). Finally, gels were stained in an ethidium bromide bath for 15 min and imaged.

Reporter Assays. A GFP reporter assay was conducted using the *E. coli* strain MKH13 (69). GFP reporter plasmids were constructed as previously described (17). Briefly, each regulatory region of interest was amplified using primers listed in Table 2 and ligated via Gibson assembly protocol with the promoterless parent vector pRU1064, which had been digested with *SpeI*, to generate reporter plasmids with GFP under the control of the regulatory region of interest. Complementary regions for Gibson assembly are indicated in lower case letters in the primer sequence (Table 2). Reporter plasmid *P_{betI}-gfp* encompasses 594-bp upstream of the *betI**BAproXWV* operon. Reporter plasmid *P_{bcct1}-gfp* encompasses 278-bp upstream of the *Pbcct1* regulatory region. Reporter plasmid *P_{bcct3}-gfp* encompasses 397-bp upstream of the *Pbcct3* regulatory region. Reporter plasmid *P_{proVI}-gfp* encompasses 438-bp upstream of the *PproVI*

regulatory region. Reporter plasmid P_{cosR} -*gfp* encompasses 397-bp upstream of the P_{cosR} regulatory region. The full-length *cosR* was then expressed from an IPTG-inducible promoter in the pBBR1MCS expression vector. Relative fluorescence (RFU) and OD₅₉₅ were measured; specific fluorescence was calculated by dividing RFU by OD₅₉₅. Strains were grown overnight with aeration at 37°C in LB1% with ampicillin (50 µg/mL) and chloramphenicol (12.5 µg/mL), washed twice with 1X PBS, then diluted 1:1000 in M9G1%. Expression of *cosR* was induced with 0.25 mM IPTG, and strains were grown for 20 hours at 37°C with aeration under antibiotic selection. GFP fluorescence was measured with excitation at 385 and emission at 509 nm in black, clear-bottom 96-well plates on a Tecan Spark microplate reader with Magellan software (Tecan Systems Inc., San Jose, CA). Specific fluorescence was calculated for each sample by normalizing fluorescence intensity to OD₅₉₅. Two biological replicates were performed for each assay.

A GFP reporter assay was conducted in RIMD2210633 wild-type, $\Delta betI$ and $\Delta opaR$ mutant strains. The P_{betI} -*gfp* reporter plasmid was transformed into *E. coli* β 2155 λ *pir* and conjugated into wild-type, $\Delta betI$ and $\Delta opaR$ mutant strains. Strains were grown overnight with aeration at 37°C in LB3% with tetracycline (1 µg/mL). Cells were then pelleted, washed two times with 1X PBS, diluted 1:100 into M9G3% and grown for 20 hours with antibiotic selection. Choline was added to a final concentration of 1 mM, where indicated. GFP fluorescence was measured with excitation at 385 and emission at 509 nm in black, clear-bottom 96-well plates on a Tecan Spark microplate reader with Magellan software (Tecan Systems Inc.). Specific fluorescence was calculated for each sample by normalizing fluorescence intensity to OD₅₉₅. Two biological replicates were performed for each assay.

Bioinformatics analysis. The *V. parahaemolyticus* protein CosR (NP_798285) was used as a seed for BLASTp to identify homologs in the *Vibrionaceae* family in the NCBI database. Sequences of representative strains were downloaded from NCBI and used in a Python-based program Easyfig to visualize gene arrangements (70). Accession numbers for select strains were: *V. parahaemolyticus* RIMD (BA00031), *V. crassotreae* 9CS106 (CP016229), *V. splendidus* BST398 (CP031056), *V. celticus* CECT7224 (NZ_FLQZ01000088), *V. lentus* 10N.286.51.B9 (NZ_MCUE01000044), *V. tasmaniensis* LGP32 (FM954973), *V. cyclitrophicus* ECSMB14105 (CO039701), *Aliivibrio fischeri* ES114 (CP000021), *A. fischeri* MJ11 (CP001133), *A. wodanis* AWOD1 (LN554847), *A. wodanis* 06/09/160 (CP039701). The *V. parahaemolyticus* RIMD2201633 CosR and *A. fischeri* ES114 EctR protein sequences were retrieved from NCBI using accession numbers NP_798285 and AAW88191.1, respectively, and input into the SWISS-MODEL workspace, which generated a 3D model of a homodimer to identify putative ligand-binding pockets (71-75).

Acknowledgements: This research was supported by a National Science Foundation grant (award IOS-1656688) to E.F.B. G.J.G. was funded in part by a University of Delaware graduate fellowship award. DPM was supported by a departmental undergraduate researcher fellowship. We thank members of the Boyd Group for constructive feedback on the manuscript.

1. Galinski EA. 1995. Osmoadaptation in bacteria. *Adv Microb Physiol* 37:272-328.
2. Csonka LN. 1989. Physiological and genetic responses of bacteria to osmotic stress. *Microbiol Rev* 53:121-47.
3. Wood JM. 2011. Bacterial osmoregulation: a paradigm for the study of cellular homeostasis. *Annu Rev Microbiol* 65:215-38.
4. da Costa MS, Santos H, Galinski EA. 1998. An overview of the role and diversity of compatible solutes in Bacteria and Archaea. *Adv Biochem Eng Biotechnol* 61:117-53.
5. Galinski EA, Oren A. 1991. Isolation and structure determination of a novel compatible solute from the moderately halophilic purple sulfur bacterium *Ectothiorhodospira marismortui*. *Eur J Biochem* 198:593-598.
6. Sleator RD, Hill C. 2002. Bacterial osmoadaptation: the role of osmolytes in bacterial stress and virulence. *FEMS Microbiol Rev* 26:49-71.
7. Roberts MF. 2004. Osmoadaptation and osmoregulation in archaea: update 2004. *Front Biosci* 9:1999-2019.
8. Roberts MF. 2005. Organic compatible solutes of halotolerant and halophilic microorganisms. *Saline Systems* 1:5.
9. Kempf B, Bremer E. 1998. Uptake and synthesis of compatible solutes as microbial stress responses to high-osmolality environments. *Arch Microbiol* 170:319-30.
10. Record MT, Jr., Courtenay ES, Cayley DS, Guttman HJ. 1998. Responses of *E. coli* to osmotic stress: large changes in amounts of cytoplasmic solutes and water. *Trends Biochem Sci* 23:143-8.
11. Wood JM. 1999. Osmosensing by bacteria: signals and membrane-based sensors. *Microbiol Mol Biol Rev* 63:230-62.

12. Naughton LM, Blumerman SL, Carlberg M, Boyd EF. 2009. Osmoadaptation among *Vibrio* species and unique genomic features and physiological responses of *Vibrio parahaemolyticus*. *Appl Environ Microbiol* 75:2802-10.
13. Ongagna-Yhombi SY, Boyd EF. 2013. Biosynthesis of the osmoprotectant ectoine, but not glycine betaine, is critical for survival of osmotically stressed *Vibrio parahaemolyticus* cells. *Appl Environ Microbiol* 79:5038-49.
14. Louis P, Galinski EA. 1997. Characterization of genes for the biosynthesis of the compatible solute ectoine from *Marinococcus halophilus* and osmoregulated expression in *Escherichia coli*. *Microbiology* 143 (Pt 4):1141-9.
15. Lo CC, Bonner CA, Xie G, D'Souza M, Jensen RA. 2009. Cohesion group approach for evolutionary analysis of aspartokinase, an enzyme that feeds a branched network of many biochemical pathways, p 594-651, *Microbiol Mol Biol Rev*, vol 73.
16. Widderich N, Hoppner A, Pittelkow M, Heider J, Smits SH, Bremer E. 2014. Biochemical properties of ectoine hydroxylases from extremophiles and their wider taxonomic distribution among microorganisms. *PLoS One* 9:e93809.
17. Gregory GJ, Morreale DP, Carpenter MR, Kalburge SS, Boyd EF. 2019. Quorum sensing regulators AphA and OpaR control expression of the compatible solute ectoine biosynthesis operon. *Appl Environ Microbiol* 85.
18. Shikuma NJ, Davis KR, Fong JN, Yildiz FH. 2013. The transcriptional regulator, CosR, controls compatible solute biosynthesis and transport, motility and biofilm formation in *Vibrio cholerae*. *Environ Microbiol* 15:1387-99.

- 538 19. Roberts MF, Lai MC, Gunsalus RP. 1992. Biosynthetic pathways of the osmolytes N
539 epsilon-acetyl-beta-lysine, beta-glutamine, and betaine in *Methanohalophilus* strain FDF1
540 suggested by nuclear magnetic resonance analyses. *J Bacteriol* 174:6688-93.
- 541 20. Lai MC, Yang DR, Chuang MJ. 1999. Regulatory factors associated with synthesis of the
542 osmolyte glycine betaine in the halophilic methanoarchaeon *Methanohalophilus*
543 *portucalensis*. *Appl Environ Microbiol* 65:828-33.
- 544 21. Nyssölä A, Kerovuo J, Kaukinen P, Weymarn Nv, Reinikainen T. 2000. Extreme
545 Halophiles Synthesize Betaine from Glycine by Methylation. *J Biol Chem*. 275:22196-
546 201.
- 547 22. Waditee R, Tanaka Y, Aoki K, Hibino T, Jikuya H, Takano J, Takabe T. 2003. Isolation
548 and functional characterization of N-methyltransferases that catalyze betaine synthesis
549 from glycine in a halotolerant photosynthetic organism *Aphanothece halophytica*. *J Biol*
550 *Chem* 278:4932-42.
- 551 23. Lu WD, Chi ZM, Su CD. 2006. Identification of glycine betaine as compatible solute in
552 *Synechococcus* sp. WH8102 and characterization of its N-methyltransferase genes
553 involved in betaine synthesis. *Arch Microbiol* 186:495-506.
- 554 24. Kimura Y, Kawasaki S, Yoshimoto H, Takegawa K. 2010. Glycine betaine
555 biosynthesized from glycine provides an osmolyte for cell growth and spore germination
556 during osmotic stress in *Myxococcus xanthus*. *J Bacteriol* 192:1467-70.
- 557 25. Landfald B, Strom AR. 1986. Choline-glycine betaine pathway confers a high level of
558 osmotic tolerance in *Escherichia coli*. *J Bacteriol* 165:849-55.

26. Andresen PA, Kaasen I, Styrvold OB, Boulnois G, Strom AR. 1988. Molecular cloning, physical mapping and expression of the bet genes governing the osmoregulatory choline-glycine betaine pathway of Escherichia coli. J Gen Microbiol 134:1737-46.
27. Lamark T, Rokenes TP, McDougall J, Strom AR. 1996. The complex bet promoters of Escherichia coli: regulation by oxygen (ArcA), choline (BetI), and osmotic stress. J Bacteriol 178:1655-62.
28. Rokenes TP, Lamark T, Strom AR. 1996. DNA-binding properties of the BetI repressor protein of Escherichia coli: the inducer choline stimulates BetI-DNA complex formation. J Bacteriol 178:1663-70.
29. Ongagna-Yhombi SY, McDonald ND, Boyd EF. 2015. Deciphering the role of multiple betaine-carnitine-choline transporters in the Halophile *Vibrio parahaemolyticus*. Appl Environ Microbiol 81:351-63.
30. Eshoo MW. 1988. lac fusion analysis of the bet genes of Escherichia coli: regulation by osmolarity, temperature, oxygen, choline, and glycine betaine. J Bacteriol 170:5208-15.
31. Scholz A, Stahl J, de Berardinis V, Muller V, Averhoff B. 2016. Osmotic stress response in Acinetobacter baylyi: identification of a glycine-betaine biosynthesis pathway and regulation of osmoadaptive choline uptake and glycine-betaine synthesis through a choline-responsive BetI repressor. Environ Microbiol Rep 8:316-22.
32. van Kessel JC, Rutherford ST, Cong JP, Quinodoz S, Healy J, Bassler BL. 2015. Quorum sensing regulates the osmotic stress response in *Vibrio harveyi*. J Bacteriol 197:73-80.
33. Chaparian RR, Olney SG, Hustmyer CM, Rowe-Magnus DA, van Kessel JC. 2016. Integration host factor and LuxR synergistically bind DNA to coactivate quorum-sensing genes in *Vibrio harveyi*. Mol Microbiol 101:823-40.

34. Ventosa A, Nieto JJ, Oren A. 1998. Biology of Moderately Halophilic Aerobic Bacteria. *Microbiol Mol Biol Rev* 62:504-44.
35. Oren A. 1999. Bioenergetic aspects of halophilism. *Microbiol Mol Biol Rev* 63:334-48.
36. Wood JM. 2007. Bacterial osmosensing transporters. *Methods Enzymol* 428:77-107.
37. Culham DE, Henderson J, Crane RA, Wood JM. 2003. Osmosensor ProP of *Escherichia coli* Responds to the Concentration, Chemistry, and Molecular Size of Osmolytes in the Proteoliposome Lumen. *Biochemistry*, 42(2):410-20.
38. Rübenhagen R, Morbach S, Krämer R. 2001. The osmoreactive betaine carrier BetP from *Corynebacterium glutamicum* is a sensor for cytoplasmic K⁺. *EMBO J*, 20: 5412-20.
39. van der Heide T, Stuart MC, Poolman B. 2001. On the osmotic signal and osmosensing mechanism of an ABC transport system for glycine betaine. *EMBO J*, 20:7022-32,.
40. Cairney J, Booth IR, Higgins CF. 1985. Osmoregulation of gene expression in *Salmonella typhimurium*: proU encodes an osmotically induced betaine transport system. *J Bacteriol* 164:1224-32.
41. May G, Faatz E, Villarejo M, Bremer E. 1986. Binding protein dependent transport of glycine betaine and its osmotic regulation in *Escherichia coli* K12. *Mol Gen Genet* 205:225-33.
42. Kempf B, Bremer E. 1995. OpuA, an osmotically regulated binding protein-dependent transport system for the osmoprotectant glycine betaine in *Bacillus subtilis*. *J Biol Chem* 270:16701-13.
43. Mahmood NA, Biemans-Oldehinkel E, Patzlaff JS, Schuurman-Wolters GK, Poolman B. 2006. Ion specificity and ionic strength dependence of the osmoregulatory ABC transporter OpuA. *J Biol Chem* 281:29830-9.

44. Chen C, Beattie GA. 2007. Characterization of the osmoprotectant transporter OpuC from *Pseudomonas syringae* and demonstration that cystathionine-beta-synthase domains are required for its osmoregulatory function. *J Bacteriol* 189:6901-12.
45. Lucht JM, Bremer E. 1994. Adaptation of *Escherichia coli* to high osmolarity environments: osmoregulation of the high-affinity glycine betaine transport system proU. *FEMS Microbiol Rev* 14:3-20.
46. Gul N, Poolman B. 2013. Functional reconstitution and osmoregulatory properties of the ProU ABC transporter from *Escherichia coli*. *Mol Membr Biol* 30:138-48.
47. Lamark T, Kaasen I, Eshoo MW, Falkenberg P, McDougall J, Strom AR. 1991. DNA sequence and analysis of the bet genes encoding the osmoregulatory choline-glycine betaine pathway of *Escherichia coli*. *Mol Microbiol* 5:1049-64.
48. Ziegler C, Bremer E, Kramer R. 2010. The BCCT family of carriers: from physiology to crystal structure. *Mol Microbiol* 78:13-34.
49. Mustakhimov, II, Reshetnikov AS, Glukhov AS, Khmelenina VN, Kalyuzhnaya MG, Trotsenko YA. 2010. Identification and characterization of EctR1, a new transcriptional regulator of the ectoine biosynthesis genes in the halotolerant methanotroph *Methylobacterium alcaliphilum* 20Z. *J Bacteriol* 192:410-7.
50. Mustakhimov, II, Reshetnikov AS, Khmelenina VN, Trotsenko YA. 2009. EctR--a novel transcriptional regulator of ectoine biosynthesis genes in the haloalcaliphilic methylotrophic bacterium *Methylophaga alcalica*. *Dokl Biochem Biophys* 429:305-8.
51. Mustakhimov, II, Reshetnikov AS, Fedorov DN, Khmelenina VN, Trotsenko YA. 2012. Role of EctR as transcriptional regulator of ectoine biosynthesis genes in *Methylophaga thalassica*. *Biochemistry (Mosc)* 77:857-63.

52. Perera IC, Grove A. 2010. Molecular mechanisms of ligand-mediated attenuation of DNA binding by MarR family transcriptional regulators. *J Mol Cell Biol* 2:243-54.
53. Sulavik MC, Gambino LF, Miller PF. 1995. The MarR repressor of the multiple antibiotic resistance (mar) operon in *Escherichia coli*: prototypic member of a family of bacterial regulatory proteins involved in sensing phenolic compounds. *Mol Med* 1:436-46.
54. Cohen SP, Hachler H, Levy SB. 1993. Genetic and functional analysis of the multiple antibiotic resistance (mar) locus in *Escherichia coli*. *J Bacteriol* 175:1484-92.
55. Hong M, Fuangthong M, Helmann JD, Brennan RG. 2005. Structure of an OhrR-ohrA operator complex reveals the DNA binding mechanism of the MarR family. *Mol Cell* 20:131-41.
56. Kumarevel T, Tanaka T, Umehara T, Yokoyama S. 2009. ST1710-DNA complex crystal structure reveals the DNA binding mechanism of the MarR family of regulators. *Nucleic Acids Res* 37:4723-35.
57. Dolan KT, Duguid EM, He C. 2011. Crystal structures of SlyA protein, a master virulence regulator of *Salmonella*, in free and DNA-bound states. *J Biol Chem* 286:22178-85.
58. Hao Z, Lou H, Zhu R, Zhu J, Zhang D, Zhao BS, Zeng S, Chen X, Chan J, He C, Chen PR. 2014. The multiple antibiotic resistance regulator MarR is a copper sensor in *Escherichia coli*. *Nat Chem Biol* 10:21-8.
59. Deochand DK, Grove A. 2017. MarR family transcription factors: dynamic variations on a common scaffold. *Crit Rev Biochem Mol Biol* 52:595-613.

60. Czech L, Hermann L, Stoveken N, Richter AA, Hoppner A, Smits SHJ, Heider J, Bremer E. 2018. Role of the Extremolytes Ectoine and Hydroxyectoine as Stress Protectants and Nutrients: Genetics, Phylogenomics, Biochemistry, and Structural Analysis. *Genes* (Basel) (4). pii: E177.
61. Reshetnikov AS, Khmelenina VN, Mustakhimov, II, Kalyuzhnaya M, Lidstrom M, Trotsenko YA. 2011. Diversity and phylogeny of the ectoine biosynthesis genes in aerobic, moderately halophilic methylotrophic bacteria. *Extremophiles* 15:653-63.
62. Shao Z, Deng W, Li S, He J, Ren S, Huang W, Lu Y, Zhao G, Cai Z, Wang J. 2015. GlnR-Mediated Regulation of ectABCD Transcription Expands the Role of the GlnR Regulon to Osmotic Stress Management. *J Bacteriol* 197:3041-7.
63. Pastor JM, Bernal V, Salvador M, Argandona M, Vargas C, Csonka L, Sevilla A, Iborra JL, Nieto JJ, Canovas M. 2013. Role of central metabolism in the osmoadaptation of the halophilic bacterium *Chromohalobacter salexigens*. *J Biol Chem* 288:17769-81.
64. Whitaker WB, Parent MA, Naughton LM, Richards GP, Blumerman SL, Boyd EF. 2010. Modulation of responses of *Vibrio parahaemolyticus* O3:K6 to pH and temperature stresses by growth at different salt concentrations. *Appl Environ Microbiol* 76:4720-9.
65. Horton RM HH, Ho SN, Pullen JK, Pease LR. 1989. Engineering hybrid genes without the use of restriction enzymes: gene splicing by overlap extension. *Gene* 77:61-68.
66. Gibson DG. 2011. Enzymatic assembly of overlapping DNA fragments. *Methods Enzymol* 498:349-61.
67. Pfaffl MW. 2001. A new mathematical model for relative quantification in real-time RT-PCR. *Nucleic Acids Res* 29:e45.

68. Kalburge SS, Carpenter MR, Rozovsky S, Boyd EF. 2017. Quorum Sensing Regulators Are Required for Metabolic Fitness in *Vibrio parahaemolyticus*. *Infect Immun* 85:e00930-16.
69. Haardt M, Kempf B, Faatz E, Bremer E. 1995. The osmoprotectant proline betaine is a major substrate for the binding-protein-dependent transport system ProU of *Escherichia coli* K-12. *Mol Gen Genet* 246:783-6.
70. Sullivan MJ, Petty NK, Beatson SA. 2011. Easyfig: a genome comparison visualizer. *Bioinformatics* 27:1009-10.
71. Waterhouse A, Bertoni M, Bienert S, Studer G, Tauriello G, Gumienny R, Heer FT, de Beer TAP, Rempfer C, Bordoli L, Lepore R, Schwede T. 2018. SWISS-MODEL: homology modelling of protein structures and complexes. *Nucleic Acids Res* 46:W296-w303.
72. Guex N, Peitsch MC, Schwede T. 2009. Automated comparative protein structure modeling with SWISS-MODEL and Swiss-PdbViewer: a historical perspective. *Electrophoresis* 30 Suppl 1:S162-73.
73. Bienert S, Waterhouse A, de Beer TA, Tauriello G, Studer G, Bordoli L, Schwede T. 2017. The SWISS-MODEL Repository-new features and functionality. *Nucleic Acids Res* 45:D313-d319.
74. Benkert P, Biasini M, Schwede T. 2011. Toward the estimation of the absolute quality of individual protein structure models. *Bioinformatics* 27:343-50.
75. Bertoni M, Kiefer F, Biasini M, Bordoli L, Schwede T. 2017. Modeling protein quaternary structure of homo- and hetero-oligomers beyond binary interactions by homology. *Sci Rep* 7:10480.

76. Makino K, Oshima K, Kurokawa K, Yokoyama K, Uda T, Tagomori K, Iijima Y, Najima M, Nakano M, Yamashita A, Kubota Y, Kimura S, Yasunaga T, Honda T, Shinagawa H, Hattori M, Iida T. 2003. Genome sequence of *Vibrio parahaemolyticus*: a pathogenic mechanism distinct from that of *V. cholerae*. Lancet 361:743-9.
77. Dehio C, Meyer M. 1997. Maintenance of broad-host-range incompatibility group P and group Q plasmids and transposition of Tn5 in *Bartonella henselae* following conjugal plasmid transfer from *Escherichia coli*. J Bacteriol 179:538-40.
78. Philippe N, Alcaraz JP, Coursange E, Geiselmann J, Schneider D. 2004. Improvement of pCVD442, a suicide plasmid for gene allele exchange in bacteria. Plasmid 51:246-55.
79. Kovach ME, Phillips RW, Elzer PH, Roop RM, 2nd, Peterson KM. 1994. pBBR1MCS: a broad-host-range cloning vector. Biotechniques 16:800-2.
80. Karunakaran R, Mauchline TH, Hosie AH, Poole PS. 2005. A family of promoter probe vectors incorporating autofluorescent and chromogenic reporter proteins for studying gene expression in Gram-negative bacteria. Microbiology 151:3249-56.

Table 1. Strains and Plasmids

Strain	Genotype or description	Reference or Source
<i>Vibrio</i>		
<i>parahaemolyticus</i>		
RIMD2210633	O3:K6 clinical isolate, Str ^r	(64, 76)
$\Delta cosR$	RIMD2210633 $\Delta cosR$ (VP1906), Str ^r	(17)
$\Delta betI$	RIMD2210633 $\Delta betI$ (VPA1114), Str ^r	This study
SSK2516 ($\Delta opaR$)	RIMD2210633 $\Delta opaR$ (VP2516), Str ^r StrR	(68)
<i>Escherichia coli</i>		
DH5 α λpir	$\Delta lac pir$	ThermoFisher Scientific
$\beta 2155 \lambda pir$	$\Delta dapA::erm pir$ for bacterial conjugation	(77)
BL21(DE3)	Expression strain	ThermoFisher Scientific
MKH13	MC4100 ($\Delta betTIBA$) $\Delta (putPA)101$ $\Delta (proP)2 \Delta (proU)$; Sp ^r	(69)
Plasmids		
pDS132	Suicide plasmid; Cm ^R Cm ^r ; SacB	(78)
pBBR1MCS	Expression vector; <i>lacZ</i> promoter; Cm ^r CmR	(79)
pBBRcosR	pBBR1MCS harboring full-length <i>cosR</i> (VP1906)	(17)
pRU1064	promoterless- <i>gfp</i> UV, Amp ^R Amp ^r , Tet ^R Tet ^r , IncP origin	(80)
pRUpectA	pRU1064 with <i>PectA-gfp</i> , Amp ^r , Tet ^r AmpR, TetR	(17)
pRUPbetI	pRU1064 with <i>PbetI-gfp</i> , Amp ^r , Tet ^r AmpR, TetR	This study
pRUPbcct1	pRU1064 with <i>Pbcct1-gfp</i> , Amp ^r , Tet ^r AmpR, TetR	This study
pRUPbcct3	pRU1064 with <i>Pbcct3-gfp</i> , Amp ^r , Tet ^r AmpR, TetR	This study
pRUPproVI	pRU1064 with <i>PproV-gfp</i> , Amp ^r , Tet ^r AmpR, TetR	This study
pRUPcosR	pRU1064 with <i>PcosR-gfp</i> , Amp ^r , Tet ^r AmpR, TetR	(17)
pET28a+	Expression vector, 6xHis; Kan ^R Kan ^r	Novagen
pETcosR	Pet28a+ harboring <i>cosR</i> , Kan ^R Kan ^r	(17)

713 **Table 2. Primers used in this study**

Use	Sequence (5'-3')	bp
Mutant		
VPbetIA	gcttcttctagaggtaccgcatgcGCCAGTTTATGTGCTCACC	580
VPbetIB	atattttatgagaCATCCCCACCTTTGGCATTTTG	
VPbetIC	gatgcctgaaCTCGACAAGCAGCTAACG	688
VPbetID	ggagagctcgatatcgcatgcTCTGCCCTACCCGGTAATC	
VPbetIFLWd	AGCATAGCACATAAGAGTCG	1895
VPbetIFLRev	CCTGATTCGCCAGTGAACGA	
EMSA		
VPbetIFwdA	CGGTTTTCTGATTTTCAGGC	125
VPbetIRevA	CTTTTAATGATAAATCGTTTGAGTTCG	
VPbetIFwdB	ATGCCAAAAATTTAGTTCGAAC	112
VPbetIRevB	GGTCTTTGAATGGATGGTAGGG	
VPbetIFwdC	CCCTACCATCCATTCAAAGACC	142
VPbetIRevC	CTAAGGCTTCTACATTGCTTTC	
VPbetIFwdD	GAAAGCAATGTAGAAGCCTTAG	202
VPbetIRevD	GAACCTGGATATGCGTCCATT	
VPbetIFwdE	AATGGACGCATATCCAAGTTC	158
VPbetIRevE	AGCATAGCACATAAGAGTCG	
VPbct1FwdA	ACCGCAAACCTCCCGATC	120
VPbct1RevA	CGGTATTCAGTACAAAAGAA	
VPbct1FwdB	TTCTTTTGTACTGAATACCG	110
VPbct1RevB	TGTCTTCAACTCACAGAAT	
VPbct1FwdC	ATTCTTGTGAGTTGAAGACA	101
VPbct1RevC	AGCGAATTTTATCACCAATCACA	
VPbct3FwdA	CGCTTTTTGTAAATGCAAATTACC	107
VPbct3RevA	CCCGTGAAAGCGGAAGATC	
VPbct3FwdB	GATCTTCCGCTTTCACGGG	108
VPbct3RevB	TCTATACCCTTTGTCATCGTTTCTC	
VPcosRFwdA	CAAATCTCCACACCATTAAATTAG	105
VPcosRRevA	CGTCTTTGGTGATTTCTTTTTATTCTG	
VPcosRFwdB	GCGAATAAAAAGAAATCACCAAAGACG	142
VPcosRRevB	CCAATTTTTTTCATCCAGTCTGTAGGG	
VPproU1FwdA	TCTTTATTCCATGCGTTG	160
VPproU1RevA	AGAGGCAGAAAGAACAGTGAA	
VPproU1FwdB	TTCACTGTTCTTTCTGCCTCT	134
VPproU1RevB	GGTTATGAATGTGTTTCGTTTGT	
VPproU1FwdC	ACAAACGAACACATTCATAACC	108
VPproU1RevC	TGGCTTGGCTTATTGGTGTTT	
VPproU1FwdD	GAACACCAATAAGCCAAGCCA	109
VPproU1RevD	GGGATCCATGTTAATTGTCTTTG	
VPbct2Fwd	ACCGAGACATGCCAATTTCTG	233
VPbct2Rev	CGGTGCTCACGAATAATCTCC	
VPbct4Fwd	AGAACAGGTTGGCTCAATGT	244
VPbct4Rev	TTCCCCTCACATCAAGTCG	
Expression		
PbetIFwd	TCTAAGCTTGCATAGCACATAAGAGTCGC	594
PbetIRev	TATACTAGTTTTGCGTCCTTGTTATTTTAAATTG	
Pbct1Fwd	tagatagagagagagagaAAACCGCAAACCTCCCGATC	278

Pbcct1Rev	actcattttttctctccaCAATCACAAATTTATGCAAAAATGAC	
Pbcct3Fwd	tagatagagagagagagagaAATTTTTTCATCCAGTCTGTAGG	397
Pbcct3Rev	actcattttttctctccaCGTTCCTCTCTATTTTGTATTATTTTTTC	
PproU1Fwd	tagatagagagagagagagaTCTTTATTCCATGCGTTG	438
PproU1Rev	actcattttttctctccaGTTAATTGTCTTTGTATGTG	
PcosRFwd	tagatagagagagagagagaCGTTCCTCTCTATTTTGTATTATTTTTTC	397
PcosRRev	cggccgctctagaactagtTATTCTGGTTTGGTGATG	
RT-PCR primers		
VPbcct1Fwd	GTTCGGTCTTGCGACTTCTC	246
VPbcct1Rev	CCCATCGCAGTATCAAAGGT	
VPbcct2Fwd	AACAAAGGGTTGCCACTGAC	167
VPbcct2Rev	TTCAAACCTGTTGCTGCTTG	
VPbcct3Fwd	TGGACGGTATTCTACTGGGC	202
VPbcct3Rev	CGCCTAACTCGCCTACTTTG	
VPectAFwd	TCGAAAGGGAAGCGCTGAG	125
VPectARev	AGTGCTGACTTGGCCATGAT	
VPasp_ectFwd	CGATGATTCCATTCGCGACG	126
VPasp_ectRev	GTCATCTCACTGTAGCCCCG	
VPproV1Fwd	GCATCGTTTCTCTCGACTCC	163
VPproV1Rev	TGCTCATCGACTACTGGCAC	
VPAbcct4Fwd	CAAGGCGTAGGCCGCATGGT	234
VPAbcct4Rev	ACCGCCACGATGCTGAACC	
VPAbetIFwd	ACTTCGGTGgTAAGCATGGG	138
VPAbetIRev	TGCCGTCAATAATGGCGTTG	
VPAbetBFwd	TGGAAATCAGCACCAGCACT	160
VPAbetBRev	TCTGCCCTACCCGGTAATCA	
VPaproXFwd	TTCCTTGGTAACTGGATGCC	216
VPaproXRev	ATCGTTACCTGGTTCGATGC	
VPaproWFwd	ATCACAGCGGCACTGGCTTGG	190
VPaproWRev	GGCGATGCGCTGCCATGATC	
16SFwd	ACCGCCTGGGGAGTACGGTC	234
16SRev	TTGCGCTCGTTGCGGGACTT	

714

715

716

717

718

719

720

721

722

Figure legends

Figure 1. RNA was isolated from RIMD2210633 after growth in M9G1% and M9G3% at an OD₅₉₅ of 0.45. Expression analysis of (A) *ectA*, *asp_ect*, (B) *betI*, *betB*, *proX2*, *proW2* (C) *bcct1*, *bcct2*, *bcct3*, *bcct4* and *proVI* by quantitative real time PCR (qPCR). 16S was used for normalization. Expression levels shown are levels in M9G1% relative to M9G3%. Mean and standard error of two biological replicates are shown. Statistics were calculated using a Student's t-test (*, $P < 0.05$; **, $P < 0.01$; ***, $P < 0.001$).

Figure 2. RNA was isolated from RIMD2210633 and $\Delta cosR$ after growth in M9G1% at an OD₅₉₅ of 0.45. Expression analysis of (A) *ectA*, *asp_ect*, (B) *betI*, *betB*, *proX2*, *proW2* (C) *bcct1*, *bcct2*, *bcct3*, *bcct4* and *proVI* by qPCR. 16S was used for normalization. Expression levels shown are levels in $\Delta cosR$ relative to wild-type. Mean and standard error of two biological replicates are shown. Statistics were calculated using a Student's t-test (*, $P < 0.05$; **, $P < 0.01$).

Figure 3. (A) The regulatory region of *betI**B**A**proXWV* was divided into five probes for EMSAs, *PbetI* A-E, 125-bp, 112-bp, 142-bp, 202-bp and 158-bp, respectively. The regulatory region used for the GFP reporter assay is indicated with a bracket. (B) An EMSA was performed with purified CosR-His (0 to 0.62 μ M) and 30 ng of each *PbetI* probe, with DNA:protein molar ratios of 1:0, 1:1, 1:5, and 1:10. (C) A *P_{betI}-gfp* reporter assay was performed in *E. coli* strain MKH13 containing an expression plasmid with full-length *cosR* (*pcosR*). Specific fluorescence of the CosR-expressing strain was compared to a strain harboring empty expression vector. Mean and standard deviation of two biological replicates are shown. Statistics were calculated using a Student's t-test (***, $P < 0.001$).

Figure 4. (A) The regulatory region of *bcct1* was divided into three similarly sized probes for EMSAs, *Pbcct1* A-C, 120-bp, 110-bp, and 101-bp, respectively. The regulatory region used for the GFP reporter assay is indicated with a bracket. **(B)** An EMSA was performed with purified CosR-His (0 to 0.69 μ M) and 30 ng of *Pbcct1* probe with DNA:protein molar ratios of 1:0, 1:1, 1:5, and 1:10. **(C)** A *P_{bcct1}-gfp* reporter assay was performed in *E. coli* strain MKH13 containing an expression plasmid with full-length *cosR* (*pcosR*). Specific fluorescence of the CosR-expressing strain was compared to a strain harboring empty expression vector (pBBR1MCS). Mean and standard deviation of two biological replicates are shown. Statistics were calculated using a Student's t-test (**, $P < 0.01$).

Figure 5. (A) A 196-bp portion of the regulatory region of *bcct3* was split into two probes for EMSAs, *Pbcct3* A and B, 108-bp and 107-bp, respectively. The regulatory region used for the GFP reporter assay is indicated with a bracket. **(B)** An EMSA was performed with purified CosR-His (0 to 0.65 μ M) and 30 ng of *Pbcct3* probe with DNA:protein molar ratios of 1:0, 1:1, 1:5, and 1:10. **(C)** *P_{bcct3}-gfp* reporter assay was performed in *E. coli* strain MKH13 containing an expression plasmid with full-length *cosR* (*pcosR*). Specific fluorescence of the CosR-expressing strain was compared to a strain harboring empty expression vector (pBBR1MCS). Mean and standard deviation of two biological replicates are shown. Statistics were calculated using a Student's t-test (**, $P < 0.01$). **(D)** An EMSA was performed with CosR-His (0 to 0.18 μ M) and probes of the regulatory regions of *bcct2* and *bcct4*. Each lane contains 30 ng of DNA and DNA:protein molar ratios of 1:0, 1:1, 1:5, and 1:10.

Figure 6. (A) The 447-bp regulatory region of the *proVI* gene was divided into four probes for EMSAs, *PproVI* A-D, 160-bp, 134-bp, 108-bp and 109-bp, respectively. The regulatory region used for the GFP reporter assay is indicated with a bracket. **(B)** An EMSA was performed with

purified CosR-His (0 to 0.64 μ M) and 30 ng of each *P_{proVI}* probe with DNA:protein molar ratios of 1:0, 1:1, 1:5, and 1:10. (C) A reporter assay was conducted in *E. coli* MKH13 harboring the *P_{proVI}-gfp* reporter plasmid and the expression plasmid *pcosR*. Specific fluorescence of the CosR-expressing strain was compared to an empty vector strain. Mean and standard deviation of two biological replicates are shown. Statistics were calculated using a Student's t-test (*, $P < 0.05$).

Figure 7. (A) A 220-bp section of the regulatory region of *cosR* was split into two similarly sized probes for EMSAs, *P_{cosR}* A and B, 105-bp and 142-bp, respectively. The regulatory region used for the GFP reporter assay is indicated with a bracket. (B) An EMSA was performed with increasing concentrations of purified CosR-His (0 to 0.66 μ M) and 30 ng of each probe with DNA:protein molar ratios of 1:0, 1:1, 1:5, and 1:10. (C) A *P_{cosR}-gfp* reporter assay was performed in *E. coli* strain MKH13 the *pcosR* expression plasmid. Specific fluorescence of the CosR-expressing strain was compared to a strain harboring empty expression vector. Mean and standard deviation of two biological replicates are shown.

Figure 8. (A) Expression of a *P_{betI}-gfp* transcriptional fusion reporter in wild-type and a Δ *betI* mutant. Relative fluorescence intensity (RFU) and OD₅₉₅ were measured after growth in (A) M9G3% or (B) M9G3% with the addition of choline. Specific fluorescence was calculated by dividing RFU by OD. Mean and standard deviation of two biological replicates are shown. Statistics were calculated using a Student's t-test (*, $P < 0.05$). (C) A reporter assay was conducted in *E. coli* MKH13 using the *P_{betI}-gfp* reporter plasmid and an expression plasmid with full-length *betI* (*pbetI*). The specific fluorescence was calculated and compared to a strain with an empty expression vector (pBBR1MCS). Mean and standard deviation of two biological replicates are shown. Statistics were calculated using a Student's t-test (***, $P < 0.001$).

Figure 9. (A) Expression of a P_{betI} -*gfp* transcriptional fusion reporter in wild-type and $\Delta opaR$ mutant strains. Relative fluorescence intensity (RFU) and OD₅₉₅ were measured after growth in M9G3%. Specific fluorescence was calculated by dividing RFU by OD. Mean and standard deviation of two biological replicates are shown. Statistics were calculated using a one-way ANOVA with a Tukey-Kramer *post hoc* test (**, $P < 0.01$). **(B)** An EMSA was performed with 30 ng of each *PbetI* probe A-E utilized previously in the CosR EMSA and purified OpaR protein (between 0.47 and 0.82 μ M) in a 1:20 molar ratio of DNA:protein.

Figure 10. Schematic of the genomic context of CosR homologs from select Vibrionaceae species. Open reading frames are designated by arrows.

Table 1. Strains and plasmids used in this study

Table 2. Primers used in this study

809

810

811

812

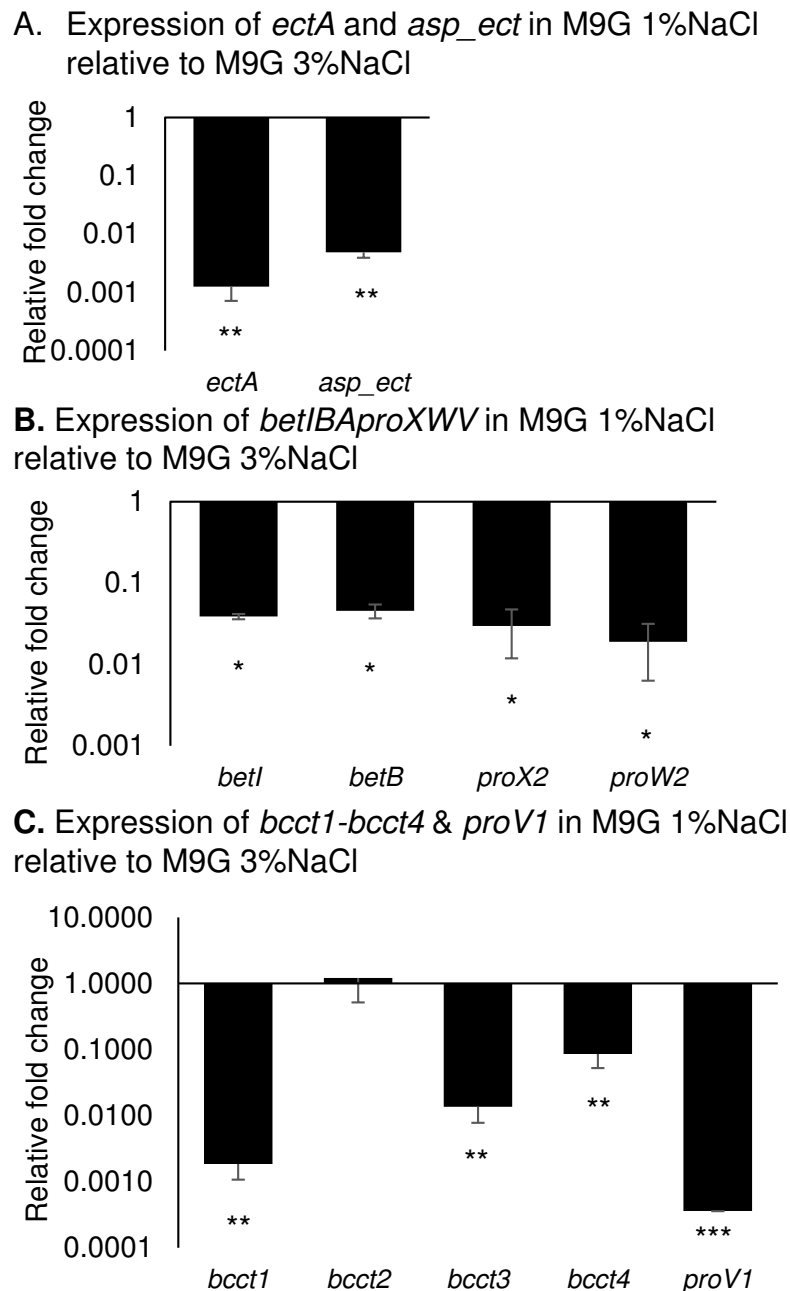
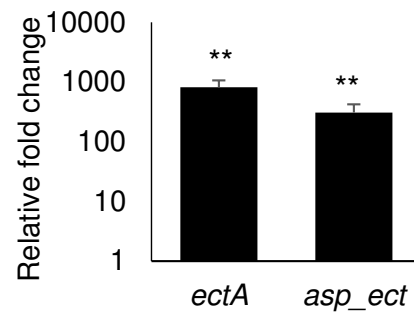
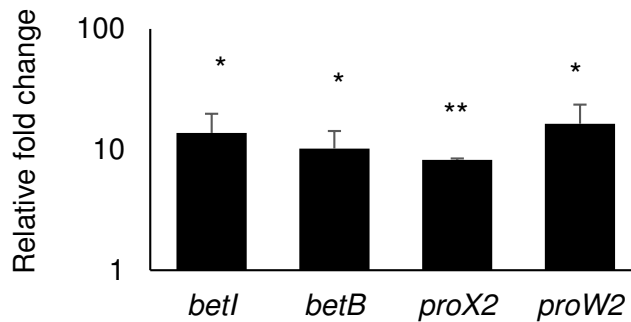


Figure 1. RNA was isolated from RIMD2210633 after growth in M9G1% and M9G3% at an OD₅₉₅ of 0.45. Expression analysis of (A) *ectA*, *asp_ect*, (B) *betI*, *betB*, *proX2*, *proW2* (C) *bcct1*, *bcct2*, *bcct3*, *bcct4* and *proV1* by quantitative real time PCR (qPCR). 16S was used for normalization. Expression levels shown are levels in M9G1% relative to M9G3%. Mean and standard error of two biological replicates are shown. Statistics were calculated using a Student's t-test (*, P < 0.05; **, P < 0.01; ***, P < 0.001).

A. Expression of *ectA* and *asp_ect* in ΔcosR relative to WT in M9G1%



B. Expression of *betI**B**aproXWV* in ΔcosR relative to WT in M9G1%



C. Expression of *bccts* and *proV1* in ΔcosR relative to WT in M9G1%

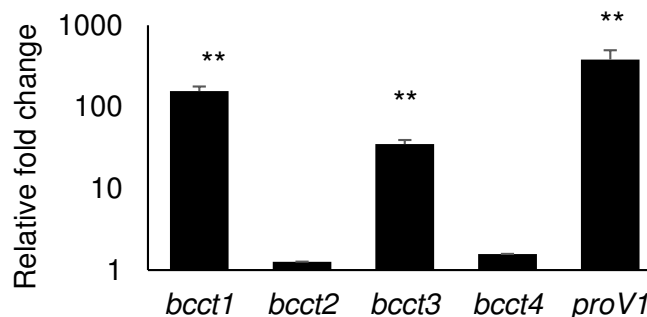
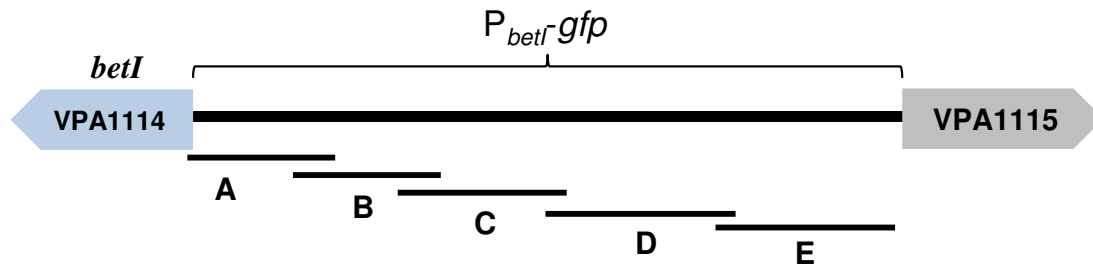
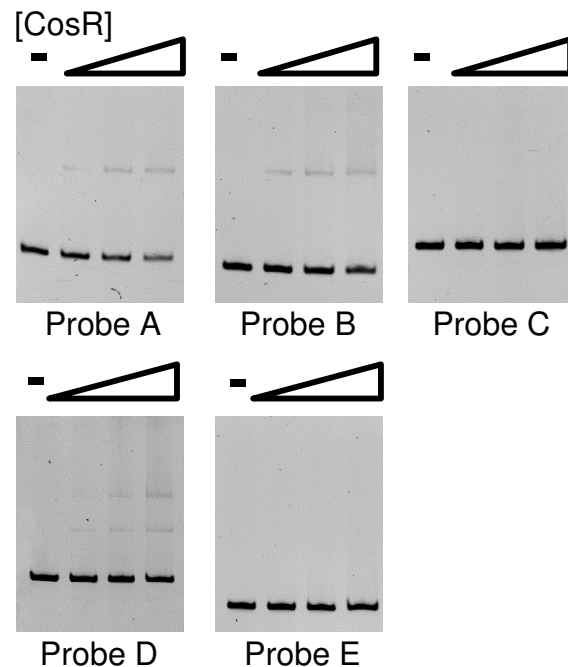


Figure 2. RNA was isolated from RIMD2210633 and ΔcosR after growth in M9G1% at an OD₅₉₅ of 0.45. Expression analysis of (A) *ectA*, *asp_ect*, (B) *betI*, *betB*, *proX2*, *proW2* (C) *bcct1*, *bcct2*, *bcct3*, *bcct4* and *proV1* by qPCR. 16S was used for normalization. Expression levels shown are levels in ΔcosR relative to wild-type. Mean and standard error of two biological replicates are shown. Statistics were calculated using a Student's t-test (*, P < 0.05; **, P < 0.01).

A. *betI* *AprXWV* regulatory region



B. *P_{betI}* CosR EMSA



C. *P_{betI}-gfp* reporter assay in *E. coli*

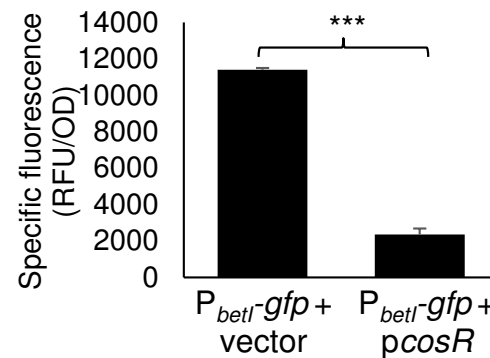
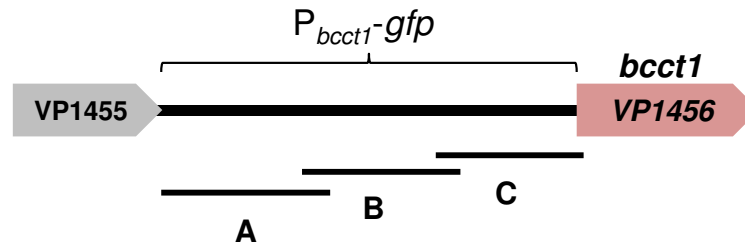
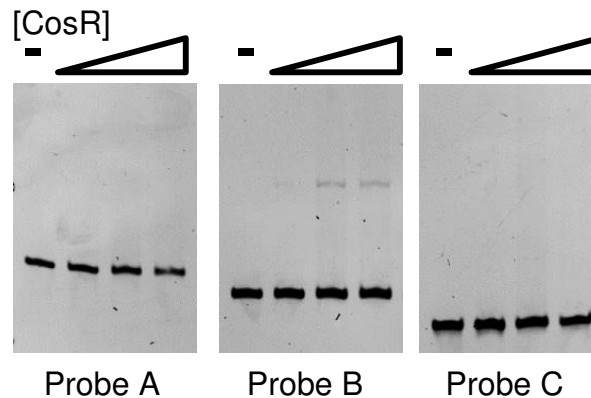


Figure 3. (A) The regulatory region of *betI* *AprXWV* was divided into five probes for EMSAs, *P_{betI}* A-E, 125-bp, 112-bp, 142-bp, 202-bp and 158-bp, respectively. The regulatory region used for the GFP reporter assay is indicated with a bracket. (B) An EMSA was performed with purified CosR-His (0 to 0.62 μ M) and 30 ng of each *P_{betI}* probe, with DNA:protein molar ratios of 1:0, 1:1, 1:5, and 1:10. (C) A *P_{betI}-gfp* reporter assay was performed in *E. coli* strain MKH13 containing an expression plasmid with full-length *cosR* (*pcosR*). Specific fluorescence of the CosR-expressing strain was compared to a strain harboring empty expression vector. Mean and standard deviation of two biological replicates are shown. Statistics were calculated using a Student's t-test (***, $P < 0.001$).

A. *bcct1* regulatory region



B. *Pbcct1* CosR EMSA



C. *P_{bcct1}-gfp* reporter assay in *E. coli*

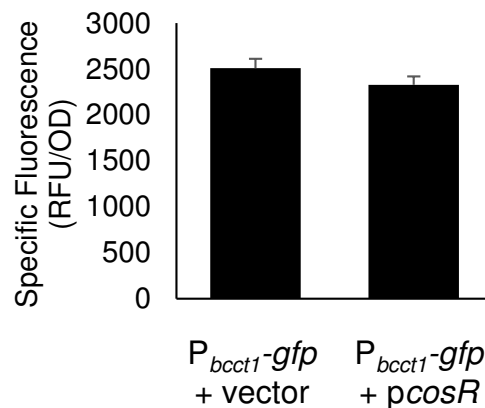
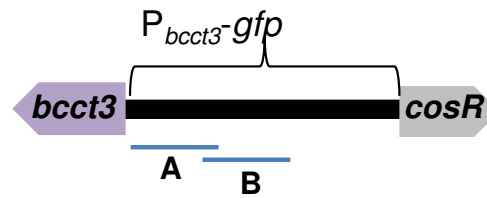
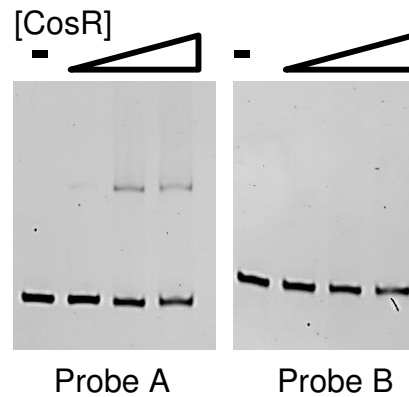


Figure 4. (A) The regulatory region of *bcct1* was divided into three similarly sized probes for EMSAs, *Pbcct1* A-C, 120-bp, 110-bp, and 101-bp, respectively. The regulatory region used for the GFP reporter assay is indicated with a bracket. (B) An EMSA was performed with purified CosR-His (0 to 0.69 μ M) and 30 ng of *Pbcct1* probe with DNA:protein molar ratios of 1:0, 1:1, 1:5, and 1:10. (C) A *P_{bcct1}-gfp* reporter assay was performed in *E. coli* strain MKH13 containing an expression plasmid with full-length *cosR* (*pcosR*). Specific fluorescence of the CosR-expressing strain was compared to a strain harboring empty expression vector (pBBR1MCS). Mean and standard deviation of two biological replicates are shown. Statistics were calculated using a Student's t-test (**, $P < 0.01$).

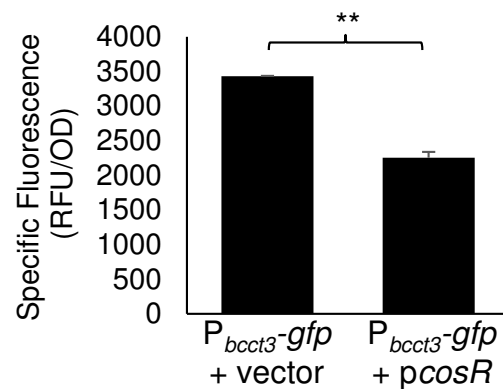
A. *bcct3* regulatory region



B. *Pbcct3* CosR EMSA



C. *P_{bcct3-gfp}* reporter assay in *E. coli*



D. *Pbcct2* and *Pbcct4* CosR EMSA

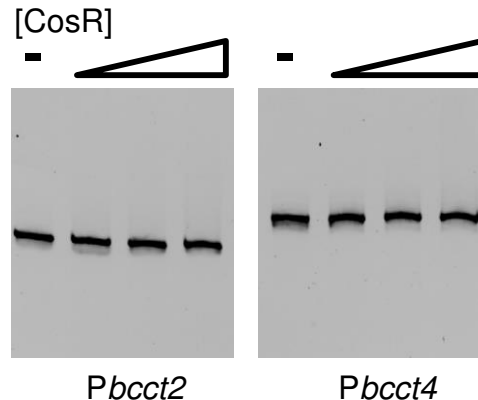


Figure 5. (A) A 196-bp portion of the regulatory region of *bcct3* was split into two probes for EMSAs, *Pbcct3* A and B, 108-bp and 107-bp, respectively. The regulatory region used for the GFP reporter assay is indicated with a bracket. (B) An EMSA was performed with purified CosR-His (0 to 0.65 μ M) and 30 ng of *Pbcct3* probe with DNA:protein molar ratios of 1:0, 1:1, 1:5, and 1:10. (C) *P_{bcct3-gfp}* reporter assay was performed in *E. coli* strain MKH13 containing an expression plasmid with full-length *cosR* (*pcosR*). Specific fluorescence of the CosR-expressing strain was compared to a strain harboring empty expression vector (pBBR1MCS). Mean and standard deviation of two biological replicates are shown. Statistics were calculated using a Student's t-test (**, $P < 0.01$). (D) An EMSA was performed with CosR-His (0 to 0.18 μ M) and probes of the regulatory regions of *bcct2* and *bcct4*. Each lane contains 30 ng of DNA and DNA:protein molar ratios of 1:0, 1:1, 1:5, and 1:10.

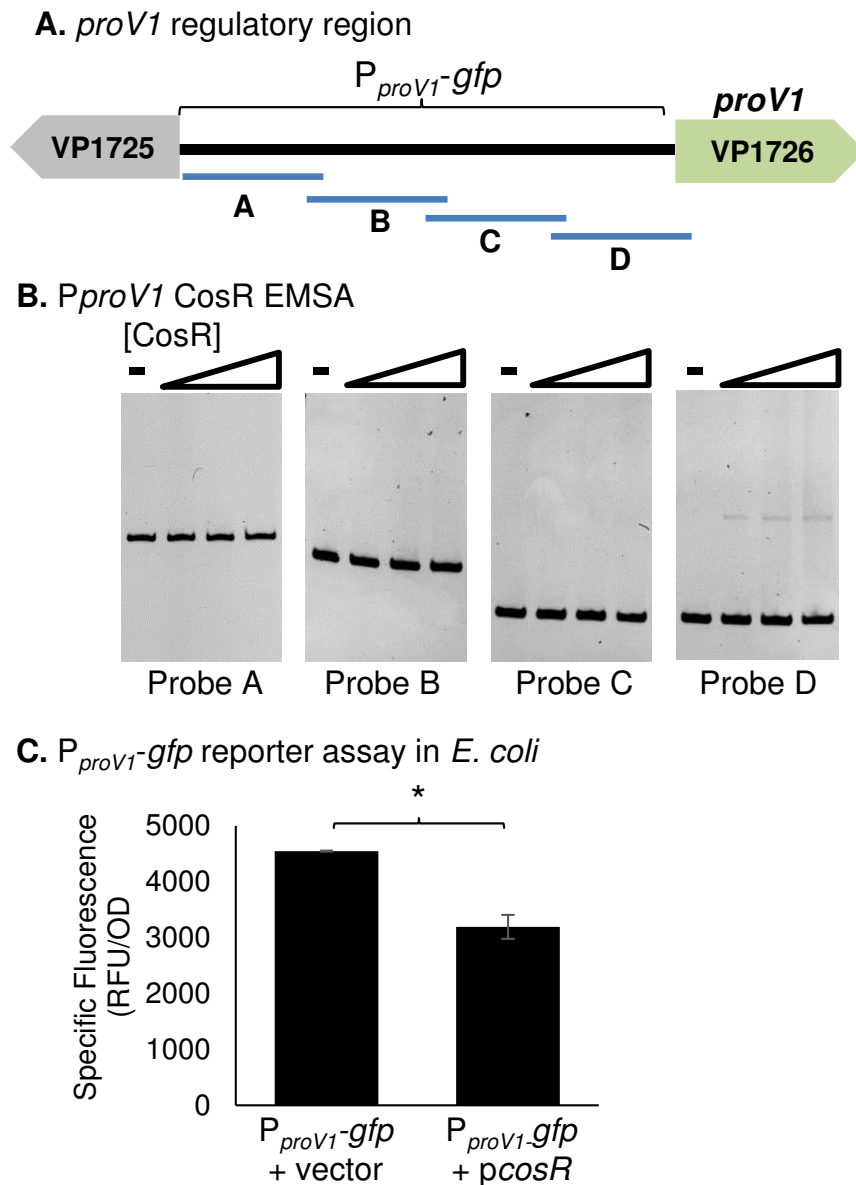


Figure 6. (A) The 447-bp regulatory region of the *proV1* gene was divided into four probes for EMSAs, *P_{proV1}* A-D, 160-bp, 134-bp, 108-bp and 109-bp, respectively. The regulatory region used for the GFP reporter assay is indicated with a bracket. (B) An EMSA was performed with purified CosR-His (0 to 0.64 μ M) and 30 ng of each *P_{proV1}* probe with DNA:protein molar ratios of 1:0, 1:1, 1:5, and 1:10. (C) A reporter assay was conducted in *E. coli* MKH13 harboring the *P_{proV1}-gfp* reporter plasmid and the expression plasmid *pcosR*. Specific fluorescence of the CosR-expressing strain was compared to an empty vector strain. Mean and standard deviation of two biological replicates are shown. Statistics were calculated using a Student's t-test (*, $P < 0.05$).

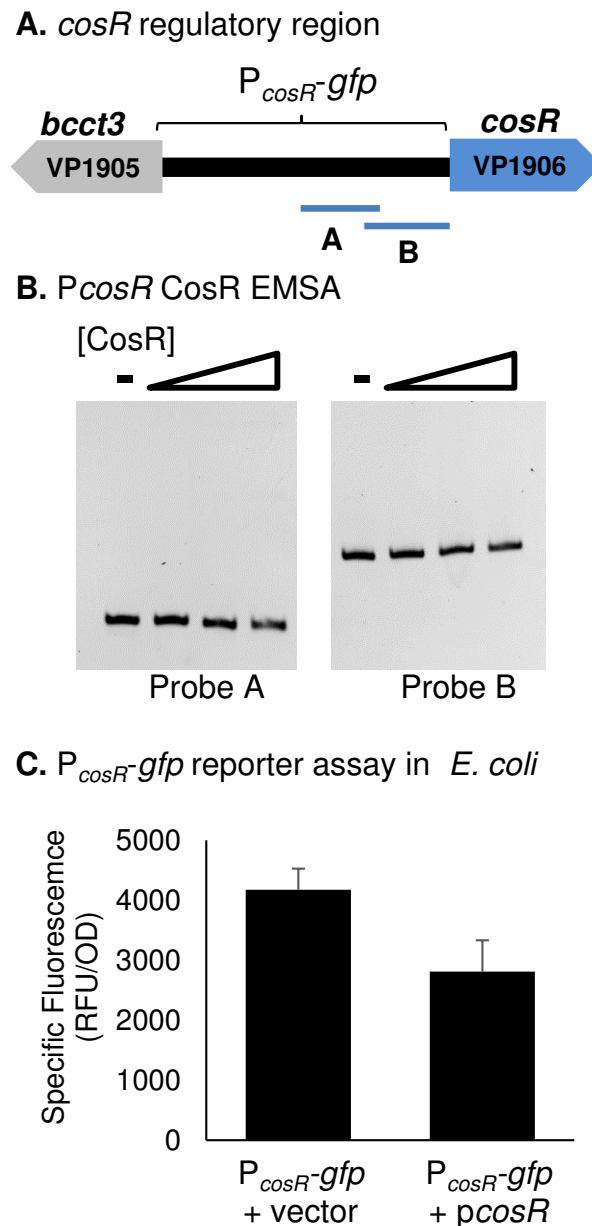
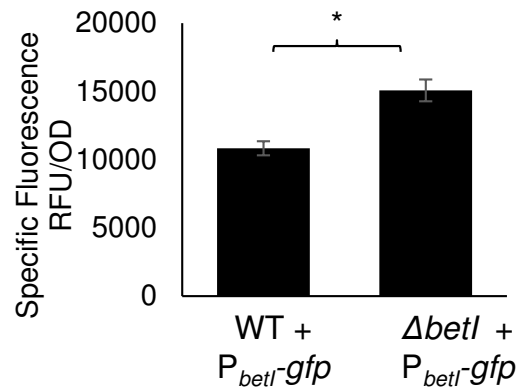
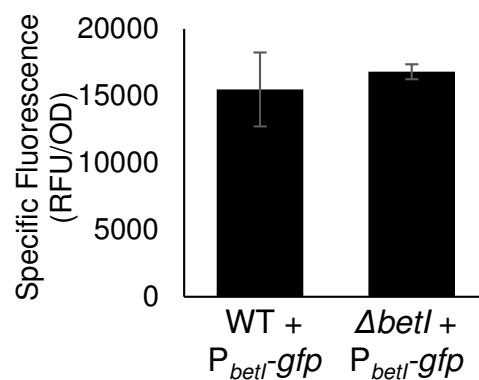


Figure 7. (A) A 220-bp section of the regulatory region of *cosR* was split into two similarly sized probes for EMSAs, P_{cosR} A and B, 105-bp and 142-bp, respectively. The regulatory region used for the GFP reporter assay is indicated with a bracket. (B) An EMSA was performed with increasing concentrations of purified CosR-His (0 to 0.66 μ M) and 30 ng of each probe with DNA:protein molar ratios of 1:0, 1:1, 1:5, and 1:10. (C) A $P_{cosR-gfp}$ reporter assay was performed in *E. coli* strain MKH13 the *pcosR* expression plasmid. Specific fluorescence of the CosR-expressing strain was compared to a strain harboring empty expression vector. Mean and standard deviation of two biological replicates are shown.

A. P_{betI} -*gfp* reporter assay
in *V. parahaemolyticus*



B. P_{betI} -*gfp* reporter assay in *V. parahaemolyticus* with choline



C. P_{betI} -*gfp* reporter assay in *E. coli*

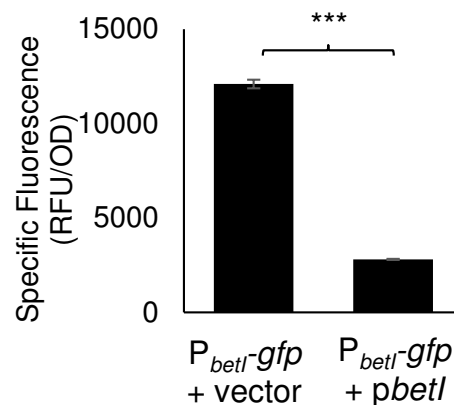
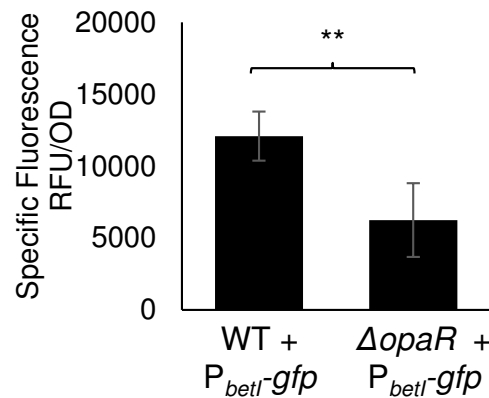


Figure 8. (A) Expression of a P_{betI} -*gfp* transcriptional fusion reporter in wild-type and a $\Delta betI$ mutant. Relative fluorescence intensity (RFU) and OD₅₉₅ were measured after growth in (A) M9G3% or (B) M9G3% with the addition of choline. Specific fluorescence was calculated by dividing RFU by OD. Mean and standard deviation of two biological replicates are shown. Statistics were calculated using a Student's t-test (*, $P < 0.05$). (C) A reporter assay was conducted in *E. coli* MKH13 using the P_{betI} -*gfp* reporter plasmid and an expression plasmid with full-length *betI* (*pbetI*). The specific fluorescence was calculated and compared to a strain with an empty expression vector (pBBR1MCS). Mean and standard deviation of two biological replicates are shown. Statistics were calculated using a Student's t-test (***, $P < 0.001$).

A. P_{betI} -gfp reporter assay in *V. parahaemolyticus*



B. P_{betI} OpaR EMSA

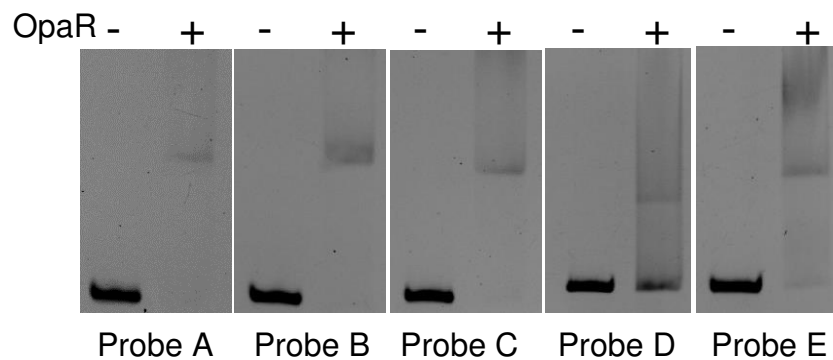
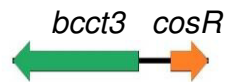
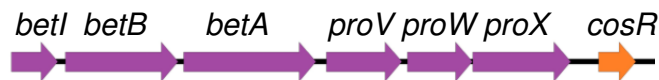


Figure 9. (A) Expression of a P_{betI} -gfp transcriptional fusion reporter in wild-type and $\Delta opaR$ mutant strains. Relative fluorescence intensity (RFU) and OD₅₉₅ were measured after growth in M9G3%. Specific fluorescence was calculated by dividing RFU by OD. Mean and standard deviation of two biological replicates are shown. Statistics were calculated using a one-way ANOVA with a Tukey-Kramer *post hoc* test (**, P < 0.01). (B) An EMSA was performed with 30 ng of each P_{betI} probe A-E utilized previously in the CosR EMSA and purified OpaR protein (between 0.47 and 0.82 μ M) in a 1:20 molar ratio of DNA:protein.

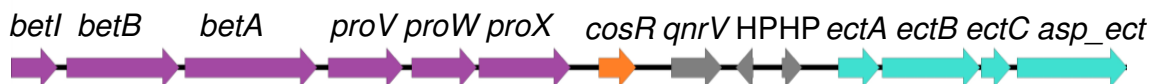
***Vibrio parahaemolyticus* and more than 50 *Vibrio* species**



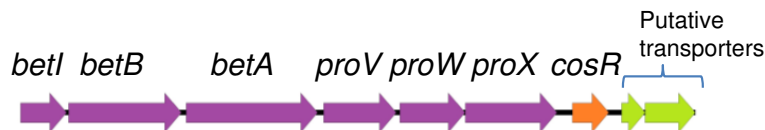
V. cyclitrophicus/V. splendidus/V. crassotreae/V. lentus/V. celticus



***Vibrio tasmaniensis/Vibrio* sp. MED222**



***A. wodanis* AWOD1/*A. wodanis* 06/09/160**



***A. wodanis* AWOD1/*A. wodanis* 06/09/160**



***A. fischeri* MJ11/*A. fischeri* ES114**



Figure 10. Schematic of the genomic context of CosR homologs from select Vibrionaceae species. Open reading frames are designated by arrows.